Accepted Manuscript

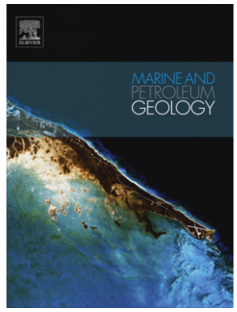

Rifting, lithosphere breakup and volcanism: Comparison of magma-poor and volcanic rifted margins

Dieter Franke

PII: S0264-8172(12)00232-2

DOI: 10.1016/j.marpetgeo.2012.11.003

Reference: JMPG 1652

To appear in: *Marine and Petroleum Geology*

Received Date: 11 July 2012

Revised Date: 19 October 2012

Accepted Date: 2 November 2012

Please cite this article as: Franke, D., Rifting, lithosphere breakup and volcanism: Comparison of magma-poor and volcanic rifted margins, *Marine and Petroleum Geology* (2012), doi: 10.1016/j.marpetgeo.2012.11.003.

Rifting, lithosphere breakup and volcanism: Comparison of magma-poor and volcanic rifted margins

Dieter Franke

Abstract

Traditionally active rifts are thought to evolve in response to thermal upwelling of the asthenosphere, whereas passive rifts develop in response to lithospheric extension driven by far-field stresses. This has often been linked to the formation of the end-member passive margin types, the volcanic, and magma-poor rifted margins. Volcanic rifted margins evolve by a combination of extension, and extensive extrusive volcanism over short time periods during breakup, manifested in reflection seismic data as seaward dipping reflectors. These margins are commonly related to mantle plumes; however, in the past years this has been questioned. Magma-poor rifted margins in contrast show wide domains of extended crust with wide-ranging extensional features as rotated faults blocks and detachment surfaces near the base of the continental crust, but limited magmatism that in addition seems to be systematically delayed to post-breakup.

In this study examples from three locations that are less frequently cited in the discussion about rifted margins being either magma-poor or volcanic in character are discussed: The Laptev Sea margin in the Arctic Ocean, where the active Arctic mid-oceanic ridge meets continental lithosphere at a high angle, the South China Sea that may represent an intermediary form of continental extension between the end member extremes, and the southernmost South Atlantic with well expressed conjugate volcanic rifted margins, which are traditionally interpreted as result of a mantle plume, the Tristan da Cunha hot-spot.

The accurate identification when continental rifting actually started and stopped, and when subsequent sea-floor spreading began is crucial information needed to refine models of margin development. Therefore, a detailed description of rift-onset and breakup unconformities is presented for the three continental margins that evolved in the Early Cretaceous, the Paleocene and the Oligocene, respectively. The examples reveal that there is no major controlling role of (hot-spot related) magmatism on the rift evolution. Instead considerable top-down control over the rift evolution and rift-related magmatism is suggested.

1. Introduction

A considerable controversy exists about the role of the mantle during rifting and the subsequent formation of oceanic crust as well as about the interaction of mantle and surface processes, i.e. the precise nature of volcanism in the rifting process.

There are two end-member extremes of passive rifted margins: (1) Volcanic rifted margins and (2) Magma-poor rifted margins A breakup of the entire crust that precedes the breakup of the lithospheric mantle is a prerequisite for the exhumation of the mantle, one of the key findings at magma-poor margins, while at volcanic rifted margins the lithospheric mantle breaks first or at the same time with the crust, resulting in the emplacement of huge amounts of syn-rift magmatic extrusives and intrusives.

In this paper, key aspects of volcanic rifted margins and magma-poor margins with respect to the role of the mantle are summarized, complemented by a description of the stratigraphic response to rifting and continental breakup; i.e. the rift-onset and breakup unconformities. As timing is essential all absolute ages are given according to Gradstein et al. (2004).

Following the rift basin nomenclature by Ziegler and Cloetingh (2004), three types of rifts and passive margins are discussed, namely (1) the active Laptev Rift in the Siberian Arctic, (2) a post-orogenic extension, which resulted in a Basin and Range type of rift, with subsequent formation of oceanic crust in the South China Sea and (3) an Atlantic-type rift in the southernmost South Atlantic, with the modern continental margins being underlain by thick wedges of volcanic flows.

1.1 Volcanic rifted margins and rift-related magmatism

Volcanic rifted margins, the majority of passive continental margins worldwide (Menzies et al., 2002; Skogseid, 2001), are characterized by thick wedges (up to 15 km) of volcanic flows (Hinz, 1981; Mutter et al., 1982) manifested in seismic reflection data as seaward dipping reflectors (SDRs), and high-velocity (V_p > 7.3 km/s) lower crust seaboard of the continental rifted margin (Fig. 1). Crustal thinning typically occurs over a comparably short distance in the order of only 50 to 100 km. The Continent-Ocean Transition (COT) is assumed to be sharp and is located in the vicinity of the SDRs (Fig. 1). Depending on the various models for the emplacement of SDRs, the COT may be placed at the seaward edge, in the center, or at the landward edge of the SDRs.

SDR wedges drilled off the British Isles during DSDP leg 81 (Roberts et al., 1984), off Norway during ODP leg 104 (Eldholm et al., 1987; Eldholm et al., 1989), and off SE Greenland during ODP legs 152 and 163 (Duncan et al., 1996; Larsen and Saunders, 1998; Larsen et al., 1994) confirmed the SDRs to be thick series of subaerial lava flows when geochemical signatures imply that the landward flows ascended through continental crust, and contrarily that the seaward flows formed in a submarine setting. The amount of interbedded sediments within the basaltic flows is unclear. However, it is possible that sediments rich in organic content were deposited within individual SDR flows during the final rifting process. In such case, given the seal quality of massive basalt flows, some of the SDR wedges may even have a petroleum potential.

Volcanic rifted margins are often associated with **large igneous provinces onshore** (Coffin and Eldholm, 1994), major regional dike swarms and sills. The magmatism occurs in geologically short time spans of ~2 Ma in the case of East Greenland and Western India (Roberts and Bally, 2012). Disregarding the difficulties in volume estimation of magmatic units which onshore are strongly affected by erosion, burial and tectonic fragmentation and which is offshore only indirectly identifiable; the offshore large igneous provinces (LIPs) (Coffin and Eldholm, 1994), the SDRs, tend in general to have the same magnitude in volume as the onshore LIPs. This has been shown for example for the US East coast margin where the total volume of igneous rocks emplaced may be as much as 2.7 x 10^6 km^3, larger than the Deccan igneous province (onshore LIP) (Kelemen and Holbrook, 1995). Gladczenko et al. (1998) estimated the volumes of the volcanic extrusives emplaced along the Argentinean/Uruguayan and the conjugate southwest African margins (offshore LIP) to be about 0.6 x 10^6 km^3; a value that is in the same order of magnitude as the original volume of the Paraná-Etendeka flood basalts (onshore LIP) which is in the range of 1.5 x 10^6 km^3 (Richards et al., 1989).

Besides the magmatic extrusives there is typically a **high-velocity lower crust** (Fig. 1) at volcanic rifted margins (Talwani and Abreu, 2000; White et al., 1987). P-wave velocities of continental lower crust seldom rise above 7.0 km/s; if so this is mainly confined to cratons or shields with a great crustal thickness (Hoolbrook et al., 1982; Rudnick and Fountain, 1995). At volcanic rifted margins, however, there is widespread lower crust showing velocities above 7.2 km/s. High-velocity lower crust is typically confined to a narrow zone in the range of about 50 km (White et al., 2008), while the extruded basalts flow for up to 200 km away from the rift. There is at present no definition about which velocity in the lower crust has to be considered as “high”. White and McKenzie (1989) predicted from lower crustal velocity of normal oceanic crust (igneous crustal thickness of 7.1 ± 0.8 km (White et al., 1992)) which has been observed to be around 6.9 km/s that velocities of 6.9 to 7.2 km/s are the possible outcome of the melting of mantle. On the other hand laboratory studies and modeling suggests that the compressional wave velocity of gabbroic rocks at the pressure and temperature of normal oceanic lower crust could be higher than 7.1 km/s (Korenaga et al., 2002). Given these uncertainties and additionally uncertainties from velocity modeling (e.g. velocity-depth ambiguity), particularly using forward modeling techniques, but owing also the nonlinear nature of tomographic inversions (Korenaga et al., 2002), a bulk lower crustal velocity above 7.2 km/s is suggested here for the interpretation of “high-velocity lower crust” unless robust uncertainty analysis for velocity models are available. Besides the hypotheses that the high-velocity lower crust originates from massive intrusions or by mafic underplating there are alternative interpretations such as partially serpentinized mantle beneath extremely stretched margins, as in the case of the Rockall Trough (O'Reilly et al., 1996) and the Porcupine Basin (Lundin and Doré, 2011), or as inherited high-grade metamorphic rocks (Ebbing et al., 2006; Gernigon et al., 2006).

The emplacement of voluminous amounts of magmatic extrusives and intrusives in short geological time spans require large and rapid amounts of melting in the mantle. This is why White (1989) proposed that an anomalously hot mantle (150-200° above normal) must be present under the rift shortly before continental breakup. In the following it has been either proposed that such temperature anomalies or mantle plumes by themselves cause the breakup of continents (e.g. Richards et al., 1989), or that hot material accumulates at the base of the lithosphere so that lithospheric thinning and decompression melting during rifting generates much greater amounts of magma than at over mantle of normal temperature (White and McKenzie, 1989). The magmatism associated with the North Atlantic volcanic rifted margins thus was proposed as being caused by passive upwelling and decompression melting of asthenospheric mantle, however, the hot mantle may have been introduced by the initiation of the Iceland plume (White, 1989). Such mantle plumes (Morgan, 1971), also referred to as hot-spots rise diapirically from the core–mantle boundary through the lower mantle and, upon reaching density equilibrium spread out variably at mantle discontinuities. This early definition has been considerably customized in the following and a wide variety of "plume" definitions are causing more confusion than precision. However, rift-plume interaction is not straight forward. The pre-rift temperature of the continental mantle and particularly the role of mantle plumes as explanation for volcanic rifting and the formation of volcanic rifted margins are under discussion. There is considerable controversy on the mechanism responsible for the production of large volumes of basaltic volcanism (Menzies et al., 2002) and over whether plumes initiate rifting, or rifting focuses plume activity (Foulger and Natland, 2003; King and Anderson, 1998; Sleep, 1971; White and McKenzie, 1989). This is because some volcanic-rifted margins cannot be directly linked to hot-spots, as e.g. the NW Australian margin and the U.S. east coast margin (van Wijk et al., 2001). Impingement of plumes on zones of crustal extension were found to variably occur almost at the same time as rifting commences (South Atlantic, Labrador Sea), after 15 Ma of rifting (Central Atlantic), some 70 Ma after the onset of rifting (Indian Ocean) or after as much as 280 Ma of intermittent crustal extension (Norwegian–Greenland Sea) (Nikishin et al., 2002; Ziegler and

Cloetingh, 2004). From the study of many intracontinental rifts Ziegler and Cloetingh (2004) concluded that initial magma generation generally occurs in the 100–200 km depth range, corresponding to the lower parts of the lithosphere and the upper asthenosphere (_ENREF_2Wilson, 1992) and only during the evolution of some rifts, an increasing contribution of melts from the asthenosphere can be recognized, both in time and generally towards the rift axis. Another finding that is difficult to be reconciled with a deep mantle origin of the melts is the along-strike segmentation of volcanic-rifted margins. Gradual changes of mantel properties and dynamics are expected to generate a smooth transition from magma starved to volcanic rifting over at least a hundred or a few hundreds of kilometers. In contrast, off Nova Scotia the North Atlantic east coast magnetic anomaly and the associated structures defining volcanic rifted margins die out and the margin is of the magma-poor type (Funck et al., 2003; Keen and Potter, 1995b). The magma-poor Bay of Biscay margin lies along strike from the volcanic rifted margins off Rockall Bank and Norway. In the volcanic rifted South Atlantic, Dragoi-Stavar and Hall (2009) found a more or less constant extent of the high-velocity lower crust along both margins, which suggests that the hot-spot influence was regionally quite limited. The transition from magma-poor to magma-rich rifting takes place within about 10 km (Franke et al., 2010). Remarkably, here the widest SDR wedges are found close to this transition, at the northern edge of the transition zone. Such abrupt change in emplaced magmatic volume argues against the hypothesis that gradual along-margin variations in the thermal regime of the lithosphere and sublithospheric mantle (the traditional plume-driven model) are solely responsible for the formation of volcanic rifted margins.

1.2 Magma-poor margins

The recovery of peridotite of the upper mantle along the Galicia margin, first by dredging in 1980, and then during ODP Leg 103 in 1987 (Boillot et al., 1980; Shipboard Scientific Party, 1987; Sibuet et al., 1987) challenged the interpretation of magma-poor margins and attracted a large number of scientists to develop new models on rifting and continental breakup, based on high quality seismic data. This finally resulted in the distinction between volcanic rifted and magma-poor margins. The term “non-volcanic margin” may be inappropriate as there is not a single passive margin that completely lacks magmatic intrusives and extrusives. The differentiation between the two end-member passive margins thus is mainly based on the volumes of magmas and a classification may not always be straight forward.

The best known examples of magma-poor margins comprise the Brazil-Angola margin (Aslanian et al., 2009; Contreras et al., 2010; Contrucci et al., 2004; Mohriak et al., 2008; Mohriak et al., 1990), the NW Australian margin (Karner and Driscoll, 2000), the Iberia-Newfoundland margin (Boillot et al., 1995; Hopper et al., 2007; Manatschal and Bernoulli, 1999; Péron-Pinvidic and Manatschal, 2009; Reston, 2007; Tucholke and Sibuet, 2007; Whitmarsh et al., 2001), and the South China Sea (Hayes and Nissen, 2005; Yan et al., 2006; Zhou et al., 1995; Zhou and Yao, 2009).

Widely discussed are polyphase faulting, depth-dependent stretching, the role and the evolution of detachment faults in combination with the nature and behavior of the lower crust, if rifting continues after the formation of first oceanic crust, and the fact that extreme crustal thinning occurred under shallow marine or even sub-aerial conditions (Clift et al., 2001; Wilson et al., 2001; Péron-Pinvidic et al., 2007; Reston, 2007; Péron-Pinvidic and Manatschal, 2009). The original crustal architecture models have been modified to acknowledge the complex architecture acquired during polyphase deformation resulting in exhumation of mantle rocks along top-basement detachment faults that carry extensional allochthons (Péron-Pinvidic and Manatschal, 2009). A basic conceptual model (initially from Boillot et al. 1980) proposes that the margin is separated into a proximal and a distal part (Fig. 1). The proximal margin is characterized by the occurrence of high-angle listric faults related to fault-bounded rift basins while the distal margin is characterized by extremely thinned crust that potentially is separated from the oceanic crust by a domain of exhumed subcontinental mantle (Mohn et al., 2012). The boundary between the two domains is at the point where the listric faults cut across the entire crust reaching the mantle (Whitmarsh et al., 2001). In the proximal margin typically a detachment is interpreted somewhere between the brittle upper crust and the mantle, while at the distal margin brittle upper crust and upper mantle are separated by only a thin lower crustal layer or are juxtaposed (Fig. 1). This leads to coupling and the development of a detachment at the crust-mantle boundary, allowing the exhumation of the mantle further seaward.

A striking observation from several magma-poor margins is that of delayed post-rift subsidence. Offshore Brazil, a salt basin developed in the South Atlantic under shallow water conditions, the Angola margin (Moulin et al., 2005), the NW Australian margin (Karner and Driscoll, 2000), the South China Sea (Franke et al., 2011), and the Iberia-Newfoundland margin (Péron-Pinvidic and Manatschal, 2009) demonstrate evidence that extremely thinned crust remained under shallow sea, or even was exposed to sub-aerial conditions for a considerable time after cessation of extension. This isostatic imbalance may argue for a considerable support from the hot asthenospheric mantle at the time when rifting ceased, a process that is not yet understood.

At the time of breakup, with the onset of seafloor spreading, magmatism becomes increasingly important at magma-poor margins. Whitmarsh et al. (2001) presented a conceptual model of a systematic oceanward increase in magmatism, both in time and space. Magmatism after the breakup of continental crust comprises in their model both, mafic intrusives and/or extrusives. This results in various amounts of emplaced magma, which are mainly confined to close to the COT.

1.3 Stratigraphic response to rifting and continental breakup

Rift-related basins and passive margins exhibit a gross stratigraphy, which, in its simplest form, may be subdivided into pre-, syn-, and post-rift sequences (Williams, 1993). A detailed rift sequence stratigraphic framework has been proposed by Martins-Neto and Catuneanu (2010).

In the following the focus will be on two major unconformities, resulting from rifting and continental breakup: (1) the rift-onset unconformity (ROU), separating the pre- from the syn-rift strata and (2) the breakup unconformity (BU), between the syn- and the post-rift strata (Fig. 2). Phases of nondeposition, and/or erosion, give rise to prominent seismic reflections, and in some cases the unconformity cuts across bedding planes of the underlying sediments resulting in angular unconformities. Unconformities generally are dated by the overlying sediments (the younger part of the unconformity), which mean that a distinct age of an unconformity is not to be correlated with the initiation of a geologic or tectonic event but with the renewed deposition following such an event.

Basically, our understanding of the nature of a rift-onset and a breakup unconformity did not change since the groundbreaking work by Falvey (1974). A **rift-onset unconformity (ROU)** (Fig. 2) results from a pre-rift or syn-rift uplift. A pre-rift uplift has classically been interpreted as the consequence of an active mantle being responsible for the induced uplift. According to Sengör and Burke (1978) volcanism likely predates rifting in this setting. In any case, the presence of a hotter than usual asthenosphere affects the subsidence experienced at the surface by (1) addition of igneous material beneath the crust and (2) the dynamic uplift of the hot mantle.

In the syn-rift case tectonic unloading may result in flexural uplift of adjacent footwall areas as the response of the lithosphere to stretching by brittle deformation in the upper crust and ductile deformation in the lower crust and mantle (Kusznir et al., 1991). Alternatively or additionally, secondary small-scale convection induced by large temperature gradients set up by rifting may be considered as explanation for the heating and the uplift.

The change from rifting to drifting and initiation of oceanic spreading is frequently marked by a prominent **breakup unconformity (BU)** (Fig. 2) (Bond et al., 1995; Falvey, 1974). This unconformity typically truncates the wedge-shaped syn-rift sediments in the rift basins separating them from the drape of post-rift sediments, and merges seaward with the top of the igneous oceanic crust. A breakup unconformity is expected to be present as an erosional unconformity at the unstretched edge of a continental margin, where it often merges with the ROU to form an amalgamation of unconformities.

The widespread occurrence of the BU in any case accounts for a short but sharp period of uplift of the rift flanks. The explanations that have been proposed for the origin of the uplift, however, remain controversial. Initially, the BU was related to a flexural rebound event that occurs at the time of continental breakup (Falvey, 1974; Miall, 2000). However, this unconformity may also be initiated by convective upwelling of the lithosphere and asthenosphere, resulting in heating and thermal expansion as a consequence of thermal heat transport, by asymmetric rifting or depth dependant stretching, as well as by isostatic imbalances. Thus, the rift-flank uplift may be explained by either a thermal imbalance or as mechanical consequence of lithospheric necking, local isostatic disequilibrium (Braun and Beaumont, 1989).

At the well studied magma-poor Iberia-Newfoundland margins, the presence of a BU has been questioned. Off Nova Scotia a prominent unconformity at the rift-to-drift transition may be lacking (Keen and Potter, 1995a) and it also has been suggested that this transition which earlier has been interpreted as breakup unconformity is rather associated with the widespread delocalization of deformation and the emplacement of alkaline magma over the conjugate deep margins rather than to the beginning of oceanic seafloor spreading (Péron-Pinvidic and Manatschal, 2009; Péron-Pinvidic et al., 2007). However, in the broad transitional zone at magma-poor rifted margins, the seafloor-spreading origin of magnetic anomalies is debated (Russell and Whitmarsh, 2003). A remnant magnetization of continental crust typically is negligible, but in the context of a rifted continental margin, there are two principal rock types which can generate substantial magnetization contrasts that give rise to magnetic anomalies. Besides mafic rocks, which make up the oceanic crust and many intrusive bodies, uppermost-mantle peridotites can acquire a significant chemical remnant magnetization, as well as an induced component of magnetization (Russell and Whitmarsh, 2003). Thus, in a magma-poor setting it may be difficult to identify true first oceanic crust in order to correlate their spreading anomalies with a breakup unconformity (Bronner et al., 2011). So far it is unclear if the problem can be solved by properly identifying the true first oceanic crust (Bronner et al., 2011) or if this needs a rethinking of the concepts that have been used to describe continental rifting and breakup of the lithosphere (e.g. Péron-Pinvidic and Manatschal, 2009).

2. Rifting and volcanism in the Laptev Sea Rift System

The Laptev Sea is one of the rare modern examples for the initial breakup of continents. It occupies the North-Eastern Siberian shelf region, where the active mid-oceanic spreading ridge (the Gakkel Ridge) meets the slope of a continental margin (Fig. 3). The tectonic and structural evolution of the Laptev Sea Rift System at the shallow shelf occurred probably in interaction with the opening of the Eurasia Basin and the evolution of the Gakkel spreading ridge, the slowest spreading segment of the actual global mid-ocean ridge system.

2.1 Regional geology

The Laptev Sea is an underexplored frontier area. Since no deep wells have been drilled on the shelves surrounding the New Siberian Islands, the precise age and nature of the sedimentary successions remains uncertain. The existence of wide and up to 15 km deep offshore rift sedimentary basins around the New Siberian Islands is proved on the basis of seismic data (Drachev et al., 1998, 1999; Franke and Hinz, 2005; Franke et al., 2001; Sekretov, 2001, 2002; Vinogradov et al., 2003). These basins are likely the sites of petroleum generation and accumulation (Cramer and Franke, 2005). However, there is discussion on the extent, tectonic style and origin of these basins. A variety of interpretations have been proposed for the sedimentary cover of the Laptev Shelf, ranging in age from the Proterozoic to the Cenozoic (Kos'ko and Trufanov, 2002). Thus, the major question is at what time interval to search for a rift-onset and a subsequent breakup unconformity.

One first order observation is that the extensional basins on the Laptev Shelf are in contrast to the widespread compressional fold belts onshore. The present-day Laptev Sea rifts are located where the Siberian Craton meets the late Permian/Early Triassic (North) Taimyr, the Late Jurassic Verkhoyansk (the widest fold-thrust belt on earth), and the late Mesozoic New Siberian-Chukchi fold belts (Fig. 3). The latter is referred to as Early Cretaceous orogeny, resulting from the late Jurassic to Early Cretaceous closure of an inferred South Anyui oceanic basin and formation of the Lyakhov-South Anyui Suture (Franke et al., 2008b; Kuzmichev, 2009; Sokolov et al., 2002). To the end of the Cretaceous period this amalgamation was in its final stage. This is manifested by studies on the Cretaceous thrusting in the Verkhoyansk Fold Belt that state that deformation ended by the Late Cretaceous (Parfenov, 2009) and by the end of granitoid plutonism and stabilization of the fold belts (Parfenov, 2009; Layer et al., 2001). From that time onwards, compression was widely replaced by extension throughout NE Siberia and the adjacent shelf areas to the north (Drachev, 2011) (Fig. 4). Our knowledge of the kinematics and history of the pre-Tertiary opening of the Arctic Ocean Basin still is limited, but the Cenozoic development of the Arctic Ocean basin is relatively well constrained. The established magnetic anomalies in the Eurasia Basin were recently updated with anomaly 2a (3.5 Ma) through anomaly 25 of Late Paleocene (58 Ma) age (Brozena et al., 2003; Glebovsky et al., 2006).

2.2 Structure of the shelf and slope and rift-related unconformities

A summary of times of hiatuses around the Laptev Sea Rift System is shown in Fig. 4 and onshore examples are presented in Fig. 5. Figure 6 illustrates an about 700 km long line-drawing interpretation across the major rift basin of the Laptev Shelf and a MCS line across the eastern Laptev Sea slope is presented in Figure 7. Across the western continental slope a couple of MCS lines were acquired by MAGE (Murmansk, Russia) (Sekretov, 2002). On the basis of available data it can be reliably stated that the margin is magma-poor. Similar to Sekretov (2002) the line across the eastern Laptev Sea slope is interpreted as imaging rotated fault blocks, bounded by deep reaching listric faults (Fig. 7); structures which are typical for magma-poor margins. Also, there are no indications for SDRs. The deep crustal structure of the Laptev Sea slope is elusive because no refractions seismic data are at hand so far. However, magma-poor rifting is also confirmed by suggested low thickness of the oceanic crust in the Eurasia Basin. Modeling of the free-water anomalies by varying the crustal thickness and average crustal density implies that if the average crustal density is less than 2900 kg/m^3, the crustal thickness must be less than 4 km (Coakley and Cochran, 1998). Both MCS lines (Figs. 6, 7) reveal a distinct rift-onset unconformity (ROU), with some evidence for erosional truncations. The breakup unconformity (BU) seals the wedge-shaped rift deposits that onlap the unconformity below and terminate against the basin-bounding listric normal faults.

Based on geology of the New Siberian Islands, it is evident that the structural pattern of pre-Cretaceous rocks is mainly due to the Early Cretaceous orogeny (Kuzmichev, 2009). The lack of compressional structures in the sedimentary strata offshore, as interpreted from seismic data (e.g. Fig. 6), thus points towards an interpretation of post-Hauterivian (Early Cretaceous) age of the rifts. After several major phases of Mesozoic compression affecting the Laptev Shelf at different angles, persistence of undisturbed earlier sedimentary basins seems doubtful. Moreover, assuming that the major part of the sedimentary fill in the Laptev Sea basins is of Mesozoic, or even Paleozoic age, the Cenozoic cover would be represented by the uppermost sedimentary succession. However, this part of the cover is widely undisturbed by faulting (Figs. 6, 7). It seems unlikely that a major rift phase resulting in seafloor spreading in the Eurasia Basin leaves an area, of less than 100 to 200 kilometres away, undisturbed.

We can also compare the width of the rift basins with the area that should be affected by extension as predicted on the basis of more globally derived extension rates from magnetic spreading anomalies in the North Atlantic and the Arctic Ocean. Summing the east-west width of the rift basins on the Laptev Shelf, a close to 600 km-wide area has been affected by extension (Franke and Hinz, 2005). This value is close to the predicted ~400 km extension from 68 to 40 Ma that had to be accommodated in northeast Siberia (Gaina et al., 2002). From the Late Cretaceous to present the Gaina et al. (2002) calculation fits the estimated

600 km of extension in the Laptev Sea region (Franke and Hinz, 2009), indicating an evolution in conjunction with the evolution of the Eurasia Basin.

Thus, a rift-onset unconformity likely has to be placed in the Cretaceous (Fig. 4). The question here is whether to interpret it at a pre-Aptian or a post-Albian position. In the Kotel'nyi Island area there is a prominent unconformity at the base of the Aptian–Albian sequence (Kos'ko and Trufanov, 2002; Kuzmichev, 2009). This corresponds on the De Long Islands to a series of unspecified erosional and structural events (Dorofeev et al., 1999) and on Bennett Island there is a missing section from the mid-Palaeozoic to the mid-Cretaceous. The hiatus observed on Belkhov Island spans from the late Paleozoic to the Paleocene (Fig. 5b). On Stolbovoi Island the youngest pre-Cenozoic are the Valanginian clastic turbitites (Kuzmichev et al., 2009).

In the coastal areas around the Laptev Shelf, the Late Cretaceous sediments have not been identified and are thus probably absent (Drachev et al., 1998). The basal unconformity above folded basement is, in some places, weathered strata which have been suggested to be related to a Late Cretaceous or Early Paleocene regional peneplain. This is supported by the presence of erosional products in Paleocene strata from granite batholiths emplaced at the end of Early Cretaceous to the beginning of Late Cretaceous in northeast Russia (Vinogradov et al., 2003). Presence of hard coal in the Aptian-Albian sequence indicates a considerable post-Early Cretaceous uplift in the Kotel'nyi Island area. The intensity of the erosional phase decreases both towards the east and towards the north (Dorofeev et al., 1999), away from the Lyakhov-South Anyui suture. Thus, a structural relationship with the Early Cretaceous orogeny is implied, rather than with the evolution of the Eurasia basin, where an increase in intensity in northern direction would be expected. Late Cretaceous strata are present on Lyakhov, on east Kotel'nyi and west Faddeya Islands (Kos'ko and Trufanov, 2002). They lie on weathered strata of the late Early Cretaceous sequence with an erosional contact. Thus there are indications that the Late Cretaceous erosional phase was most intense in the north and decreases towards the east and towards the south. This indicates that the more likely candidate for a rift-onset unconformity has to be located in the Late Cretaceous as it was earlier suggested by Drachev et al. (1998).

If we accept this stratigraphic position for the rift-onset unconformity it becomes evident that there is no distinct breakup unconformity in the area of the New Siberian Islands but obviously a hiatus that combines the rift-onset with a breakup unconformity. The initiation of the breakup unconformity (Fig. 4) is correlated here with the onset of seafloor spreading in the Eurasia Basin and with the fact that weathering and peneplanation continued up to the end of the Paleocene on the New Siberian Islands. Onshore we therefore observe an amalgamation of the breakup unconformity with the rift-onset unconformity, which is expected at the boundaries of the basin. It is obvious that the Late Cretaceous and Early Paleocene uplift was substantial and that a large region was affected by erosion despite the finding that the rift itself is magma-poor.

2.3 Magmatism during the rifting stage

This Laptev Sea Rift System can be classified as a magma-poor rift because evidence for extrusive magmatism is rare to absent in the rift basins (Figs. 6, 7) (Drachev et al., 1998; Franke et al., 2001). Exceptions are small-scale high-reflective bands on top of the acoustic basement close to the shelf break that correspond to magnetic anomalies (Fig. 3). The major parts of the New Siberian Islands, except the De Long Islands are reported to be lacking extrusive magmatism (Dorofeev et al., 1999). The De Long Province is in fact outstanding in the magnetic field data (Fig. 3). Saltus et al. (2011) classified the magnetic field around the De Long Islands as long wavelength, continuous high, wide linear zones, indicating thick mafic crust. Potentially rift related basalts are widespread on Bennett Island where the flows make up a 350-m succession (Fig. 5C). The basalts show an intraplate geochemical signature and, together with the East Spitsbergen and Franz Josef Land basalts were interpreted as part of the Early Cretaceous Arctic large igneous province (Drachev and Saunders, 2006). K–Ar whole-rock ages on Bennett Island are 124±6, 110± 5, 109±5, 106±4

Ma, constraining the age of the basaltic magmatism to the Aptian/Albian stage (Dorofeev et al., 1999; Drachev and Saunders, 2006; Kuzmichev, 2009). In the area of the De Long Islands there are additionally Neogene-Quaternary basalts reported (Dorofeev et al., 1999). The De Long volcanic province thus may be considered as surface expression of a potentially long-lived hot-spot.

2.4 Discussion on the evolution of the Laptev Sea Rift System

In summary, a hot-spot was located at the edge of the future Laptev Sea Rift System, being active about 20 Ma before breakup of the Eurasia Basin and thus being an excellent candidate to deliver breakup related basalts. But the rifting process in the Laptev Sea did not integrate the hot-spot and developed as magma-poor rift and continental margin. If we accept the proposed timing of the rift onset it is evident that a major uplift and erosional event preceded the rift phase, resulting in a widespread hiatus caused by erosion and peneplanation. Thus, we observe a major uplift despite the lack of rift-related magmatism. Onshore the breakup unconformity is likely amalgamated with the rift-onset unconformity, indicating a major erosional phase. Offshore the breakup unconformity seals the wedge-shaped rift deposits in the half-grabens and represents merely a depositional hiatus.

Rifting is ongoing nowadays, but Franke et al. (2001) concluded that the seismic refraction velocities for the Mohorovičić discontinuity (MOHO) of around 8.0 km/s and the relatively low attenuation of the shear waves for the crust and upper mantle of the Laptev Sea shelf determined from earthquake data (Franke et al., 2000) do not support a mantle driven rift system. Although there is Neogene-Quaternary volcanism reported for parts of the De Long Islands (Dorofeev et al., 1999) rifting in the Laptev Sea at present is not driven by the mantle.

3. The South China Sea - Magma-Poor Rifting

The South China Sea is one of the largest marginal seas along the western Pacific Margin (Fig. 8). Apart from the oceanic basin, the South China Sea waters cover a domain of heavily attenuated continental crust (green area in Fig. 8), which it is close in its size (more than

1000x1000 km) to the Basin and Range province in the United States. The area is particularly well suited for studying the transition from rifting to seafloor spreading because the marginal basin is relatively young and thus it likely preserves differences in subsidence and thermal history resulting from rifting. After only 10 to 15 Ma of seafloor spreading, the margins are still close enough to each other to allow detailed studies of conjugate pairs of continental margins.

3.1 Regional geology

Rifting in the South China Sea (SCS) started in the Late Cretaceous to Early Paleocene when a Mesozoic convergent margin changed to extension. The rift phases that subsequently resulted in the formation of the South China Sea started with an initial uplift of the rift shoulders followed by widespread erosion and peneplanation (Cullen et al., 2010; Ru and Pigott, 1986; Taylor and Hayes, 1980, 1983; Zhou and Yao, 2009). The origin of this extension is under discussion and there are several competing models that aim to explain the formation of the South China Sea oceanic basin. It has been suggested that during the period from 180 to 80 Ma, the slab dip angle of the subducting Paleo-Pacific plate underneath SE China increased from a very low angle to a median angle (Zhou and Li, 2000). Consequently, magmatic activity of the SE China continental margin migrated to the southeast, from 800-1000 km inland to only 100–200 km inland. Such a slab role back around greater SE Asia is suggested as origin of the early episode of extension (Doust and Sumner, 2007), however, extension as induced by the collapse of the mountain range is also a likely mechanism. In any case, it can be expected that various degrees of mantle wedge melting and basaltic underplating during the subduction provided the necessary heat to weaken the lower- and middle- crust, allowing the generation of a wide rift.

Though the age of the oceanic crust is under discussion, there is a general agreement on a decreasing age of the oceanic crust towards the southwest (Fig. 8). In the northeastern portion of the South China Sea, close to Taiwan Island, Hsu et al. (2004) interpreted Late Eocene/Early Oligocene oceanic crust (37.8 Ma to 30.1 Ma), but the nature of the crust there is ambiguous. The timing of seafloor spreading in the central South China Sea has been revised to 31–20.5 Ma by Barckhausen and Roeser (2004), from 32 to 15.5 Ma (Briais et al., 1993; Taylor and Hayes, 1983). Thus, poly-phase rifting was followed by poly-phase seafloor spreading. A key role may have played the crustal blocks of Macclesfield Bank and Reed Bank (Fig. 8). These can be considered as equivalents of the Flemish Cap and Galicia Bank at the Newfoundland/Iberia margins in the Atlantic, where these blocks are interpreted as continental microplates unaffected by internal deformations during lithosphere rupture (Hopper et al., 2007). In the South China Sea it is speculated that seafloor spreading in the southwestern portion of the South China Sea was hindered by a rigid block of continental crust (Sun et al., 2009) and only after 25 Ma of continuing rifting led to the break-up of that block into two pieces which now form Macclesfield Bank and Reed Bank (Fig. 8).

3.2 Rift-onset unconformity (ROU)

In the northeastern South China Sea continental margin, close to Taiwan Island, thick lower Cretaceous sediments (shale siltstone, sandstone) and also Jurassic sedimentary rocks were encountered (Li et al., 2008). A sharp angular ROU occurs between the Mesozoic and the Cenozoic sequences in the West Taiwan Basin (Fig. 8). The lower part of this unconformity dates generally back to the Early Cretaceous (Aptian/Albian) (c. 110 Ma), and it represents a depositional hiatus of about 50-65 Ma (Li et al., 2008; Lin et al., 2003) (Fig. 9).

According to Sun et al. (2009), rifting in the Beibu Basin initiated in the Late Cretaceous, while in the Pearl River Mouth Basin rifting initiated only in the Late Paleocene, at around 59 Ma and climaxed during the Late Eocene (Shi et al., 2011). The Qiongdongnan Basin, to the west of the Pearl River Mouth was initially rifted in the Early Eocene, at about 44 Ma. Rifting reached its peak during the Late Eocene through the Early Oligocene, with a smaller reactivation occurring in the Late Oligocene (Shi et al., 2011). Apparently the rifting migrated from east to west and from north to south and the erosional phase associated with the rift-onset decreases in magnitude from NE to SW (Fig. 9).

Offshore Vietnam, an angular unconformity between pre-Tertiary and younger deposits in the Phu Khanh Basin is interpreted as the ROU (Fyhn et al., 2009a; Fyhn et al., 2009b). Further south, only few wells penetrated the pre-rift strata and the situation is less clear. Dredge samples from the Dangerous Grounds Basin and the Reed Bank confirmed Late Triassic to Early Jurassic siltstones and shales, Late Jurassic metasediments and amphibolites, Early Cretaceous mica-schists, paragneiss and quarz phyllites (Schlüter et al., 1996), whereas Late Cretaceous strata are missing. In the NW Borneo offshore region at least two episodes of rifting have been identified (Cullen, 2010). In the Dangerous Grounds the pre-rift sedimentary unit is deformed by thrusts and the crests of some anticlines have been eroded away, implying a major hiatus (Ding et al., 2012). An Eocene regional episode of extension is recognized in Luconia and the Dangerous Grounds basin (Fig. 8) and a second, early Oligocene extensional phase lasted until the onset of seafloor spreading in the South China Sea. In the Reed Bank area and the NW Palawan shelf Early Cretaceous (and some Jurassic) sediments were encountered in drill holes (Schlüter et al., 1996) but again, Upper Cretaceous successions are apparently widely eroded (Franke et al., 2011; Sales et al., 1997). In summary, although less distinct, a mirror image of an increase in the magnitude of erosion in eastern direction can be deduced along the southern margin (Fig. 9).

3.3 Is there a breakup unconformity (BU)?

Several authors have addressed the question of an Oligocene BU around the South China Sea. This resulted in a wide variety of proposed ages for the unconformity, even at the well explored South China margin. According to biostratigraphic data from petroleum industry wells, the end of rifting can be limited to earlier than c. 28 Ma in the Pearl River Mouth basin (Clift et al., 2001). The identification of this unconformity is complicated by the fact that during the proposed breakup time there was a deep marine trough in the central South China Sea (Clift et al., 2002). Ocean drilling program (ODP) Site 1148 at the northern margin (Figs. 8 & 9) revealed bathyal water depths (>500 m) at the distal margin at the breakup time (Clift et al., 2001; Shipboard Scientific Party, 2000) and drilling on the Reed Bank has identified deep-water, clastic sedimentary rocks of Paleocene to Middle Eocene age (Taylor and Hayes, 1980). Thus, a continuously developed BU may not be expected (Montadert et al., 1979). In addition, Ru et al. (1994) and Cullen (2010) suggested from the fact that breakup was diachronous that the corresponding unconformity has to be diachronous and getting younger from east to west for about 10 Ma. This highlights the necessity to relate the age of this unconformity to specific geographical locations (Fig. 9).

Perhaps the best evidence for a breakup unconformity was found in the northeastern SCS, close to Taiwan Island, where a missing section ranges at least from 37 Ma to 30 Ma as judged by the ages of its youngest underlying and oldest overlying sediments (Lin et al., 2003). Oligocene uplift was followed by rapid, early post-breakup subsidence between c. 30-18 Ma. In the Pearl River Mouth Basin, the breakup-related hiatus was identified on the basis of biostratigraphic data from wells (Zhou et al., 1995). This provides an approximate time range for the hiatus from 33 to 32 Ma in the eastern, and from 28 to 27 Ma for the western Pearl River Mouth basin. In contrast, the ODP Site 1148 revealed the most significant unconformity not at around 30 Ma but at c. 23.8 Ma, evidenced by sharp changes in geochemical parameters, and a preceding hiatus totaling to 2.5–3 Ma (Shipboard Scientific Party, 2000). This hiatus was explained by a spreading ridge jump to the South (Shipboard Scientific Party, 2000). This timing fits well with the breakup-related hiatus from 23 to 22 Ma proposed for the Qiongdongnan Basin (Zhou et al., 1995).

In the Vietnamese Cuu Long Basin, the rifting continued until the end Oligocene time when a distinct unconformity at the Oligocene/Miocene boundary (c. 23 Ma) marks the onset of post-rift sagging (Fyhn et al., 2009a). This unconformity was interpreted as breakup-related, and was traced seaward into the Nam Con Son Basin, where it indicates the onset of a second rift phase.

In the northeastern Dangerous Grounds, the Reed Bank area and NW Palawan the BU is directly overlain by a widespread carbonate platform (Nido carbonates) and timing constraints on the age of the BU are derived mainly from the ages of these carbonates. The top of these limestones is at Lower Miocene level (c. 22 Ma to c. 17 Ma) (Hinz and Schlüter, 1985; Schlüter et al., 1996). Offshore NW Palawan the platform carbonate formation was established in the Early Oligocene (Grötsch and Mercadier, 1999) and the formation of the platform carbonates terminated about latest Oligocene times, at about 25 Ma (Franke et al., 2011). Several dredge samples of Late Oligocene to Early Miocene platform carbonates to the south and southwest of Reed Bank also confirm this interpretation (Kudrass et al., 1986). This indicates a mid-Oligocene age for the unconformity in the Reed Bank area and NW Palawan, similar to the conjugate margin off South China (Pearl River Mouth basin).

3.4 Cenozoic magmatism in the South China Sea

Yan et al. (2006) reviewed Cenozoic magmatism in the South China Sea. These authors conclude that volcanism contemporaneous with rifting and sea floor spreading in the South China Sea was very weak and that there was only very limited magmatic activity, most probably after the cessation of sea floor spreading. Minor rift-related magmatism is confirmed in the Pearl River Mouth basin, where about 20% of the wells have penetrated small-scale Paleogene igneous rocks (Yan et al., 2006), having K–Ar ages of 57–49 Ma. The clearest evidence of basalts is a 400 m thick section of Early Miocene basic igneous rocks drilled in the Pearl River Mouth Basin (well BY-7-1; Yan et al., 2001).

Widespread post-rift volcanism, which likely postdates the spreading phase, is most distinct by up to 4 km high seamounts that are aligned along the extinct spreading axis (Fig. 8). Sampling revealed alkali- and trachybasalts with ages between 11 and 3.5 Ma (Pautot, 1990; Taylor and Hayes, 1983), about 8 to 15 Ma after the cessation of seafloor spreading. The best constrained age is that of a seamount offshore Taiwan Island, where Ar–Ar dating revealed an age of 22 Ma (Hsu et al., 2004).

This falls well in the time when volcanism became increasingly active (Flower et al., 1992; Yan et al., 2006), a fact that is also reflected in the structure of the continental margins. Clift et al. (2001) pointed out, that, although there is no magmatism comparable with the seaward-dipping reflectors of volcanic rifted margins, there is seismic evidence of volcanic rocks spanning a width of c. 25 km close to the inferred oceanic crust at the northern margin. This phase of magmatism is widespread along the lower slope of the northern margin of the South China Sea, close to the Dongsha Rise (e.g. Lüdmann and Wong, 1999) and well imaged by the data shown by Hu et al. (2009) (Fig. 10). There is no age dating at hand for these volcanoes, but most of the volcanic structures are exposed to the seabed or covered by only thin deposits, indicating that they have been erupted close to recent, but definitely after the cessation of seafloor spreading.

Similar findings are reported from the southern margin, off NW Palawan (Franke et al., 2011), with the difference that these authors did not interpret the volcanic rocks as being emplaced over continental rocks and thus suggested a post-rift emplacement (Figs. 10 & 11). In fact the structures as found at the continent-ocean transition (volcanic flow unit in Fig. 11) in the South China Sea are surprisingly similar to post-rift sills overlying basement of the continent–ocean transition zone on the magma-poor Newfoundland margin (Péron-Pinvidic et al., 2010). The sill emplacement there post-dated the onset of seafloor spreading by at least 7–15 Myr as proved by drilling during ODP Leg 210. In the South China Sea case we do not have reliable dating at hand but given the similarities a post-rift emplacement seems plausible.

Further south, in the NW Borneo/Palawan Trough Franke et al. (2008a) interpreted young volcanoes (? Pliocene). Similarly basalts of Pliocene age, or younger have been dredged offshore NW Palawan (Kudrass et al., 1986). Hutchinson 2010 argues that all the conical features were carbonate built-ups but some of these reveal a distinct magnetic signal implying a magmatic origin.

Offshore Vietnam the onset of basaltic volcanism, accompanied by regional uplift occurred during the middle Miocene (Lee and Watkins, 1998). Such early Neogene volcanism is supported by an early to middle Miocene alkaline basaltic volcano drilled at the northern edge of the Phu Khanh Basin, offshore Vietnam. Fyhn et al. (2009a) stated more precisely that widespread volcanism onshore south and central Indochina postdates the early

Neogene, although a small number of basalts from central Vietnam yield Middle and Early Miocene ages.

Whether the scattered Cenozoic magmatism over and around the South China Sea and its adjacent areas shares a common origin is unclear. However, tomographic images of S-wave velocity confirm the existence of a mantle plume. Under Hainan a weak but resolved velocity perturbation is visible down to about 1900 km depth, confirming a deep mantle origin (Montelli et al., 2006). High-resolution tomographic images of the upper mantle show a tilted low-velocity conduit with a diameter of about 80 km in the upper mantle that extends from below the extinct spreading ridge towards Hainan (Lei et al., 2009). This shape is surprising because the mantle flow as induced by the Indian collision likely goes southeastward and is expected to cause a plume conduit tilt in the opposite sense of what is observed.

There is also a distinct surface expression of that hot-spot. In the northern Hainan Island region, the area of Cenozoic igneous rocks, mostly basalts, covers more than 7.000 km^2 (Flower et al., 1992). However, these basalts were neither emplaced during the rifting stage, nor during the seafloor-spreading stage. The magmatism was vigorous in the Pliocene-Recent but quiet or very weak before the Pliocene (6 Ma) (Flower et al., 1992; Yan et al., 2006).

3.5 High-velocity lower crust at magma-poor margins?

In the case of magma-poor rifting a high-velocity lower crust at continental margins is surprising. However, several papers report a high-velocity lower crust at the northern margin of the South China Sea from refraction seismic studies (Kido et al., 2001; Nissen et al., 1995; Wang et al., 2006; Yan et al., 2001). This was reported mainly along the eastern South China margin; a crustal profile across the Xisha trough, to the north of Macclesfield Bank (Fig. 8) did not reveal high-velocity lower crust (Qiu et al., 2001).

First reports on a 10 km thick high-velocity lower crust came from two-ship expanded spread profiles in 1985 (Nissen et al., 1995). In this study P-wave velocities exceeding Vp = 7.0 km/s were considered as high. These early studies have had some limitations on the data quality and the 1-D modeling approach did not completely constrain the deep crustal structure. In the following several deep seismic profiles with Ocean Bottom Seismometers or Ocean Bottom Hydrophones have been completed along the northern margin with one line being shot along a previous expanded spread-line and resulting in an average of only 4 km thick lower crust being shown with variable velocities of 7.2-7.5, or 7.1-7.3 km/s, respectively (Yan et al., 2001). Another line (OBS2001), disturbed by overlying volcanoes and igneous rocks, imaged an up to 5 km thick lower crust with velocities between 6.5 and 7.5 km/s (Wang et al., 2006). Unpublished refraction seimic studies from the southern Palawan shelf and the Spratly Islands shelf did not reveal high velocities in the lower crust (W. Ding, pers. comm.). Twenty sono-buoy measurements at the northern margin revealed only in one case crustal velocities exceeding 7.2 km/s (Guong et al., 1989). The presence of a high-velocity lower crust is apparently confirmed from the different measurements but it may be limited to the northeastern margin of the South China Sea.

3.6 Discussion on the magmatism in the South China Sea and the formation of rift-related unconformities

In the magma-poor rifted South China Sea, there is clear evidence for a widespread rift-onset unconformity (ROU) with a northeastward increasing magnitude of the related hiatus. However, the Upper Cretaceous strata are widely absent throughout the area. There is a widespread angular unconformity that characterizes the transition from the Mesozoic sequences to the Cenozoic sequences with numerous examples for erosional truncations. This is in contrast to the particular finding from Ziegler and Cloetingh (2004) that the rifts that lack of volcanic rocks or show only a very low level of volcanism are generally not associated with progressive large-radius crustal doming.

A breakup unconformity (BU) has an erosional character only at the proximal margins. The areas close to the COT were already subaquatic during breakup. If we agree with the proposed ages of the oceanic crust as derived from the interpretations of the magnetic spreading anomalies it is evident that the rift-drift unconformity in the South China Sea consistently postdates breakup by about 6 to 8 Myr (Fig. 9).

For the proposed high-velocity lower crust in the Dongsha Islands region at the northeastern margin the typical underplate model seems doubtful. Nissen et al. (1995), who performed heat flow versus subsidence modeling, concluded that assuming the high-velocity lower crust to have been produced by underplating is inconsistent with the observed modest subsidence. Instead of underplating, the high velocity crust could be explained by emplacement of intrusive magmatic bodies. Intrusion of hot basaltic magma will heat and weaken the lithosphere. With sufficient weakening, rifting should continue even if the supply of magma wanes or ends (Bialas et al., 2010). However, given the fact of extreme crustal thinning, large amounts of magmatic intrusives would be expected to also result in considerable syn-rift extrusives and this is not the case. Instead a relationship with voluminous post-rift magmatism is suggested. The Dongsha block, located in this region was initially uplifted at the Miocene/Pliocene boundary (c.5.5 Ma); close to the Hainan plume volcanism. The major post-drift uplift phases in that region have been associated with intrusion of magma into the crust (Lüdmann and Wong, 1999). It appears possible that the high-velocity lower crust has its origin in this post-drift magmatism.

4. The southern South Atlantic – the plume case?

The South Atlantic is a classical place for the correlation between continental breakup and magmatic events, resulting in a large igneous province. The voluminous Paraná–Etendeka continental flood-basalt provinces in Brazil and Namibia (Fig. 12), respectively, are commonly referred to the influence of the Tristan da Cunha hot-spot with the Walvis Ridge and Rio Grande Rise as the expression of the plume tail (Morgan, 1971; Wilson, 1963). It has been proposed that continental rifting commonly follows flood basalt volcanism (Richards et al., 1989), and it is a popular opinion that this hot-spot triggered and initiated the opening of the South Atlantic Ocean.

4.1 Regional geology

West Gondwana broke up in Early Cretaceous times and subsequent seafloor spreading resulted in the formation of the the South Atlantic Ocean. South America rotated clockwise with respect to Africa and it took almost 40 Ma, from earliest Valanginian to late Albian time, for Africa and South America to separate completely (Szatmari, 2000). The final opening of the southern South Atlantic took place in the Early Cretaceous, following the southern North Atlantic, and being followed by the Equatorial Atlantic (Jackson et al., 2000). A connection of the central and South Atlantic was established only by the latest Aptian (Bengtson and Koutsoukos, 1992). In the Maastrichian, at about 70 million years ago the orientation of the spreading between South America and Africa changed, as seen by the change of the orientation of the Walvis Ridge and the overall spreading rate slowed down. This probably came along with a major erosional phase which is manifest in the seismic data and may be linked to orogenic processes in the Andes. From that time on, the South Atlantic spreading axis began to migrate westward, away from the Tristan da Cunha hot-spot, with a resulting transition to intraplate hot-spot volcanism along the Walvis Ridge and associated termination of the Rio Grande Rise formation. Post-rift sediment thicknesses at the southern South Atlantic continental slope range between one and only few kilometers. If there is a regional Aptian/Albian marine source rock (Rehder and Franke, 2012), in areas where Tertiary contourites/turbidites (Oligocene and younger; Gruetzner et al., 2012) overly the Aptian sediments these reach maturities suitable for the formation of hydrocarbons (Grassmann et al., 2011).

Continental breakup and initial seafloor spreading in the South Atlantic were accompanied by extensive transient magmatism as inferred from sill intrusions, flood basalt sequences, voluminous volcanic wedges, and high-velocity lower crust at the present continental margins. In seismic reflection data voluminous extrusives are manifested by huge wedges of SDRs on both sides of the southern South Atlantic (Bauer et al., 2000; Blaich et al., 2011; Fernàndez et al., 2010; Franke et al., 2010; Franke et al., 2007; Gladczenko et al., 1997;

Gladczenko et al., 1998; Hinz et al., 1999; Jackson et al., 2000; Talwani and Abreu, 2000). Industry drilling off Namibia (Kudu Field) showed that the lavas were erupted subaerially (Clemson et al., 1999). The SDRs are emplaced symmetrically along the conjugate continental margins (Blaich et al., 2009; Talwani and Abreu, 2000). High-velocity lower crust was identified by all deep seismic studies in this segment of the South Atlantic (Bauer et al., 2000; Franke et al., 2006; Hirsch et al., 2009; Schnabel et al., 2008), with some indications that the volumes are larger at the eastern margin.

A finding from several volcanic margins and also from the western margin of the southern South Atlantic is the lack of the expected rift structures in the upper crust (Franke et al., 2007). To allow for crustal thinning to an amount where the crust can break and oceanic crust can be generated both, the upper and the lower crust have to be thinned considerably. While the lower crust may have thinned in a ductile manner, the upper crust is expected to be brittle. Thus, the upper crust needs to break and graben structures have to develop (Skogseid, 2001). It has been argued that the southern South Atlantic may be described in a simple-shear manner, with the rift basin (i.e. Orange and Walvis Basin) at one side only. But still, at the position of the future breakup a major graben is expected. The absence of the appropriate extensional structures may simply be an imaging problem due to the high impedance of overlying volcanic extrusives. Large volumes of basalts result in a very high impedance contrast; the ray path is distorted by velocity variations between basalt and surrounding sediment, and the uneven surface of the volcanics results in energy scattering. Still puzzling in the southern South Atlantic is the magnitude of intra-continental deformation during rifting and there is some discussion on the oldest magnetic anomalies being present in the southernmost segment of the South Atlantic. Rabinowitz and LaBrecque (1979) proposed Chron M9N (c.133 Ma) as the earliest spreading anomaly. In addition, these authors interpreted Chron M11 (c. 136 Ma) close to the Orange Basin at the African margin. Nürnberg and Müller (1991) suggested that the rift phase lasted from 150 to 130 Ma until Chron M4. Eagles (2007) and Moulin et al. (2009) questioned the presence of Chron M11 (c. 136 Ma) and suggested that only the M7 anomaly can be defined in the southern part of the

Orange Basin and the offshore Rawson Basin. It is suggested here that pre-M7 anomalies indeed are present in the southern South Atlantic (Schreckenberger et al., 2002), particularly in the southernmost segment. In the volcanic rifted segment these may be located partly within the SDR wedges (Bauer et al., 2000; Schreckenberger et al., 2002; Séranne and Anka, 2005) and not within the oceanic crust (Fig. 12).

4.2 Rift-onset unconformity (ROU)

The number of extensional phases which affected the continental shelf before the final Late Jurassic – Early Cretaceous phase of South Atlantic extension is not well understood. A summary of known ages of the onset of rifting around South Africa is given by Jackson et al. (2000). Estimations for the southern African basins are: Cape Basin, 220-200 Ma; Orange Basin, 160 Ma to 144 Ma; Lüderitz-Walvis Basins, 126 Ma (Fig. 13). The ages should be handled with caution, because the earliest rift fill was rarely drilled and these estimations may vary by as much as 20 Ma for any particular basin (Jackson et al., 2000). However, at least two phases of rifting, as suggested by Keeley and Light (1993), occurred in the Late Triassic-Early Jurassic and in the Mid-Jurassic - before the major Late Jurassic to Early Cretaceous rift phase that subsequently resulted in seafloor spreading. The continental extension may have begun in isolated centers during the Late Triassic which were located mainly along the Permian-Triassic orogenic belt (Uliana and Biddle, 1987). At that time almost all of south and west Gondwana was affected by magmatism resulting in a very high heat flow (Macdonald et al., 2003). Rifting along the southern margin of Africa progressed SW-wards in southern South America (Light et al., 1993a) following the direction of principal extensional stress that was towards the s

outhwest at this time (Tankard et al., 1995). The Late Jurassic northwest-southeast directed opening of the Weddell Sea in Antarctica at about 155 Ma (Jokat et al., 2003) offers an explanation for the presence of sedimentary basins that formed at a high angle to the present continental slope of the South Atlantic. Thus, early stages of local rifting and sedimentation may be recorded in the Colorado Basin of Argentina, the Salado Basin of Argentina and

Uruguay and the Cape Basin of South Africa. An early extensional phase may also be reflected by the lower syn-rift succession in the North Falkland Graben (Richards and Fannin, 1997). The sedimentary basins along the southern African margin are commonly attributed to the final rifting phase that began in the late Jurassic in the Orange Basin and in the Early Cretaceous in the Walvis Basin (Uliana and Biddle, 1987). Onshore the initiation of this final rifting phase is estimated by e.g. Uliana et al. (1989) and Stollhofen (1999) to occur at 160 Ma.

4.3 Breakup unconformity (BU)

The change from rifting to drifting and onset of oceanic spreading is marked by a prominent breakup unconformity (BU) that can be traced from the shallow shelves to the top of the SDRs before it merges with the top of the igneous oceanic crust (Fig. 14).

The BU (Fig. 13) is reported to be of late Valanginian age (c. 137 Ma) in the North Falkland Basin (Richards and Hillier, 2000; Ross et al., 1996) and in the Outeniqua Basin off Africa (Lawrence et al., 1999); at the boundary between Hauterivian and Barremian, at c. 130 Ma (Baldi and Nevistic, 1996) in the San Jorge Basin; of Aptian age (c. 118 Ma) in the Rawson Basin (Otis and Schneidermann, 2000); of middle Barremian age (c. 127 Ma) in the Colorado Basin (Fryklund et al., 1996; Juan et al., 1996); and of late Barremian/early Aptian age (c. 125 Ma) in the Salado (Punta del Este) Basin (Stoakes et al., 1991; Tavella and Wright, 1996). Hinz et al. (1999) proposed a minimum Hauterivian age (125 Ma according to the used time-scale), or c.133 Ma corresponding to Gradstein et al. (2004) time-scale for breakup at the Argentine margin but noted that the BU may be time transgressive. Along the southern African margin, four well defined basins developed, which are connected since the Upper Cretaceous, losing their individuality (Gerrard and Smith, 1982). In the Orange and Lüderitz basins the rift-to-drift transition is commonly interpreted at the end of the Hauterivian (Brown et al., 1995; de Vera et al., 2009; McMillan, 2003). Earlier studies proposed a Valanginian age for the BU (Gerrard and Smith, 1982). Thus, it is assumed to be of at least Hauterivian age as in the Walvis basin (Light et al., 1993b; Maslanyj et al., 1992; see also the discussion in Séranne and Anka, 2005). This is confirmed by Corner et al. (2002) who report that shallow marine limestones of Barremian age form the top of the synrift sediments and were encountered in two wells. DSDP wells drilled at the Walvis Ridge encountered the unconformity at the Barremian/Aptian boundary (Sibuet et al., 1984b). Continental breakup in the Brazilian – West-African segment is inferred to have occurred by Aptian-Albian time, at c. 112-110 Ma (Karner et al., 2003; Moulin et al., 2005; Mohirak and Leroy, 2012).

4.4 The Tristan da Cunha hot-spot and the opening of the South Atlantic

The Tristan da Cunha hot-spot is one of the rare examples meeting the characteristics of a deep plume (Courtillot et al., 2003). It reveals trap magmatism at the initiation and long-lived tracks expressed as the largest bathymetric features of the South Atlantic, the Walvis Ridge (Fig. 12) and the Rio Grande Rise. However, the seismic anomaly beneath the Tristan da Cunha hot-spot is consistently found to be confined to the upper mantle only (Foulger, 2005).

Menzies et al (2002) and Moulin et al. (2009) compiled published geochemical data and radiometric dates for the dikes and the lava flows in the Paraná–Etendeka flood-basalt provinces (Fig. 12). These compilations reveal that volcanic activity peaked in the late Hauterivian–early Barremian (133-129 Ma and 134–130 Ma, respectively). The magmatism predates the seafloor-spreading stage at the latitude of Namibia and Brazil by 5 to 10 million years (Hawkesworth et al., 1999), the uncertainty resulting mainly in identifying and dating the oldest magmatic spreading anomaly.

It is a popular opinion that the mid-Cretaceous opening of the southern South Atlantic was predated by the extrusion of the Etendeka and Paraná flood basalts (e.g. Gladczenko et al., 1997; Wilson, 1992). There are a number of findings that question this relationship. The magma flow directions of both the basaltic rocks from the Etendeka igneous province of Namibia and from the Paraná province in Brazil show essentially the same trend, implying that rifting preceded flood volcanism, at least in the portion of the magmatic province within 100 km of the nascent spreading ridge (Glen et al., 1997). Off the Namibian coast pre-Etendeka sediments were deposited in north-south–trending rift basins (Clemson et al., 1997), revealing that substantial extension occurred prior to the main phase of flood volcanism. Also dynamic modeling of continental extension between South America and Africa shows that the mechanics of rifting played an important role in determining the pattern of volcanism within the Paraná and Etendeka flood-basalt provinces (Harry and Sawyer, 1992). Geochemical studies revealed that the majority of the Paraná-Etendeka flood basalts were derived from the lithospheric mantle, while only the final alkalic magmas, postdating continental breakup, had greater contributions from the underlying asthenosphere (Hawkesworth et al., 1992; Peate et al., 1990). Thus, in the vicinity of the Paraná-Etendeka flood basalts rifting preceded the emplacement of the flood basalts and the latter were derived mainly from the shallow mantle.

Following several phases of extension the opening of the South Atlantic started at a position which was close to the evolving Falkland-Agulhas Fracture Zone, potentially in a basin that once formed the northern prolongation of the North Falkland Graben. Earlier phases of extension, possibly in relation with the northwest-southeast directed opening of the Weddell Sea in Antarctica at about 155 Ma, had resulted in previous crustal thinning. From the varying angles of extension affecting the South Atlantic rift it is suggested here that the extensional direction rotated clockwise from initially NW-SE (Late Triassic-Early Jurassic) to N-S (Middle Jurassic) before the major Late Jurassic – Early Cretaceous crustal stretching episode resulting finally in an E-W directed breakup (Fig. 15). Most important, however, is that there was a well established seafloor spreading system in the southern South Atlantic when the flood basalts were emplaced in the Paraná-Etendeka province in the late Hauterivian–early Barremian (Fig. 15B & 15C). Moulin et al. (2009) infer that the first oceanic crust in the southern area formed between M9 and M7 (between 134 and 132 Ma), in Hauterivian time. The breakup unconformity with a Valanginian age (c. 137 Ma) in the North Falkland Basin (Richards and Hillier, 2000; Ross et al., 1996), as similarly in the Outeniqua Basin off Africa (Lawrence et al., 1999) implies even Valanginian oceanic crust (Fig. 13). This confirms (1) the opening of the South Atlantic went from South to North (Austin and Uchupi, 1982; Rabinowitz and Labrecque, 1979; Sibuet et al., 1984a; Uchupi, 1989), a fact that is also confirmed by the ages of the breakup unconformities along both continental margins (Fig. 13), and (2) the, at least, Hauterivian age of the first oceanic crust, close to the Falkland-Agulhas Fracture Zone (Fig. 15). Becker et al. (2012) thus interpreted Barremian sediments on top of the earliest oceanic crust close to the Falkland-Agulhas Fracture Zone. This places the vast majority of the Etendeka and Paraná flood basalts definitely into the post-rift stage and likely into the early seafloor-spreading stage. It is thus concluded that the South Atlantic started to open at the most distal point from the inferred plume head and opened towards the plume. The contrary would be expected if an active mantle is responsible for the induced uplift and subsequent rifting (Fig. 16).

Moreover, the SDRs are not continuously emplaced along the margins of the southern South Atlantic from the Paraná-Etendeka flood basalt province to the Falkland-Agulhas Fracture Zone (FAFZ; Fig. 12). There is a strong magnetic anomaly on both sides of the southern South Atlantic that is associated with the SDRs (Large Marginal Anomaly or anomaly G; Fig. 12). Off the South African coast, the anomaly reveals much stronger amplitudes than on the Argentine side, representing an asymmetry between both margins. However, the Large Marginal Anomaly exhibits a similar sudden southern termination of the SDRs and thus the volcanic part of the rifted margin. This is confirmed by reflection seismic data (Franke et al., 2010) and reveals that at one stage during the initial opening of the South Atlantic the rift did suddenly and sharply change from magma-poor and highly volcanic rifting. Gradual changes of mantle properties and dynamics would be expected to generate a smooth transition from magma-starved to volcanic rifting over at least a hundred or a few hundreds of kilometers (Franke et al., 2010).

5. Discussion and Conclusions

5.1 The rift-onset unconformity (ROU)

Despite the presence of considerable pre-rift or syn-rift volcanism a rift-onset unconformity (ROU) is a common phenomenon in all three studied regions. Thus, there is no intrinsic relationship between pre-rift uplift and the presence of a hot-spot as suggested earlier (e.g. Campbell, 2007). Strong erosion and peneplanation is reported for the time of rift-onset for the Laptev Sea region, resulting in the absence of most of Upper Cretaceous deposits around the rift system. In the South China Sea, the rift-onset had most dramatic consequences in the northeast, where the rift initiated; however the unconformity can be followed throughout the area and it is present also close to the present COTs. Thus, not only the rift shoulders were uplifted but also the center. In the volcanic-rifted area of the South Atlantic there is no doubt about the presence of a rift-onset unconformity (Fig. 13). In the Laptev Sea Rift System the onset of rifting is not well constraint but in the other two cases there are indications that uplift occurred before the onset of major extension. This further confirms the findings of Ziegler and Cloetingh (2004), who concluded from the study of Phanerozoic rifts that doming of rift zones is basically a consequence of lithospheric extension.

5.2 The breakup unconformity (BU)

For the Iberia-Newfoundland magma-poor margins, the concept of a breakup unconformity has been questioned. Also beneath large parts of the northern continental margin of the Bay of Biscay, the change from magma-poor rifting to subsequent seafloor spreading took place in Early Cretaceous time in a pre-existing marine basin so that deep syn-rift sediments grade, without interruption, to deep post-rift sediments in half grabens. This setting resembles the South China Sea area, where the areas close to the COT were already subaquatic during breakup. In this case, one cannot expect a continuous breakup unconformity (Montadert et al., 1979).

In the South China Sea area there is in addition a problem in correlating the breakup unconformity with the age of the adjacent oceanic crust. If we agree with the proposed ages of the oceanic crust as derived from the interpretations of the magnetic spreading anomalies it is evident that the rift-drift unconformity in the South China Sea postdates breakup by about 6 to 8 Myr (Fig. 9). Similarly, in the Atlantic Newfoundland-Iberia rift existing interpretations placed the 'breakup unconformity' some 15 Ma younger than the oldest magnetic anomaly, and it is 9 Ma younger than confident oceanic crust (Tucholke et al., 2007). Tucholke et al. (2007) suggested that consistent accretion of 'normal' oceanic correlates with the historically proposed breakup unconformity, a view that is shared by Bronner et al. (2011), who pointed out that exhumed mantle, which is variably intruded by igneous rocks, is difficult to distinguish from ‘normal’ oceanic crust in magnetic and seismic data. In the South China Sea this would mean that vast part of what now is interpreted as oceanic crust from magnetic spreading anomalies would merely be exhumed continental mantle, which is highly intruded by igneous rocks. However, this concept is probably not applicable for the South China Sea rift, which likely did not reach sufficient thinning to enter the stage of mantle exhumation in its major part (Franke et al., 2011; Ding et al., 2012). In addition to existing concepts that have been used to describe continental rifting and breakup of the lithosphere to the 3-D nature of rifting has to be considered. The V-shaped oceanic crusts (Fig. 8), as well as southwestward decreasing ages for the BU are an indication that the early phase of seafloor spreading is related to an oceanic propagator. In a conceptual 3D evolution model (Fig. 17) seafloor spreading at one location coincides with continuing rifting further along-strike the future margins. A breakup of the next rift segment, with a flexural roll-back or an induced thermal anomaly thus overprints the area that already is in the seafloor spreading stage. Such 3D breakup pattern could reflect the evolution of the corresponding unconformity and may explain the delay in the formation of the BU in the case of oceanic propagators. An uplift event is suggested to not only influence the margins on both sides of the rift but also the evolving oceanic basin with its passive margins behind the progressing rift.

5.3 Is high-velocity lower crust always breakup related?

The syn-rift nature of the high-velocity lower crust at the northern South China Sea margin is questioned here. From the timing of the magmatism in this region it appears plausible to propose a formation well in the seafloor-spreading stage, or when seafloor spreading ceased. A high-velocity lower crust may not only be reflecting structure inheritance of crustal domains and features related to older tectonic episodes but may also evolve late, during the seafloor spreading stage. It may also be speculated that there is a relationship between high-velocity lower crustal bodies and regional uplift resulting potentially in mantle delamination and forced melting, as e.g. in the Dongsha Island region, South China Sea, or the South African continental margin in the South Atlantic. Further deep seismic studies are needed to validate such a hypothesis.

However, if high-velocity lower crustal bodies are confirmed to originate on occasion, or partly during post-rift times, rift-related magmatism may have been overestimated at passive margins. Studies that estimate potential mantle temperatures from the volumes of the magmatic intrusives at breakup time typically take the instantaneous emplacement of such magmatic features for granted. However, as most passive margins experienced substantial post-drift uplift a delayed emplacement of high-velocity lower crustal material cannot be excluded.

5.4. Some remarks on the origin of melts

Besides the temperature of the mantle, inherited structures, and the localization of thinning, among others, the velocity at which breakup propagates certainly influences the melt supply.

In the examples studied here, rift propagation velocity shows not much difference. In the southern South Atlantic breakup propagated c. 1.500 km within c. 12 Myr, at a velocity of c. 12 cm/yr. In the South China Sea breakup propagated c. 1300 km within 14 Myr, i.e. at about 9 cm/yr. However, in the South China Sea initial seafloor spreading is reported as slow, with half-spreading rates ranging between only 0.25 and 0.45 cm/yr (Barckhausen and Roeser, 2004; Briais et al., 1993; Hsu et al., 2004). Magnetic lineations in the southern South Atlantic in contrast show by a factor of ten higher half spreading rates of 2.4 - 3.4 cm/yr for pre-M2 oceanic crust (Schreckenberger et al., 2002). Thus a relationship between initial spreading rates and the volumes of melts is implied.

In addition it is proposed here that the structure of the lithosphere, and particularly discontinuities, or transfer zones, strongly influence the generation of melts. In the South China Sea, the volcanism that is manifested in the COT-area is apparently concentrated at the seaward edge of crustal blocks, e.g. Dongsha, Reed Bank and the Northwest Palawan Block (Franke et al., 2011). These blocks were not thinned to the same amount as the interjacent areas. Similarly, at the magma-poor Newfoundland margin, major sills were emplaced seaward of a crustal block (H-block; Péron-Pinvidic et al., 2010). The magmatism occurred likely during the early seafloor-spreading stage with a well established shallow mantle convection system. Such coincidence at two different magma-poor margins may imply a common origin and may point to edge-effect volcanism. In this view, the deep-reaching roots of continental blocks modify small-scale convection cells in the mantle that were initiated by passive upwelling and decompression melting and attract more volumes of melts to seaboard of the crustal blocks rather than at the highly attenuated portions of the continental margins.

To explain the formation of volcanic rifted margins Armitage et al. (2010) suggested that predominantly the localization of thinning of the lithosphere focuses melt into the breakup region and thus controls the melting rather than the mantle temperature. In the following, such localized rifting is combined with transfer zones that hinder rift propagation. A lithosphere scale is suggested for the transfer zones which are suggested to decouple individual rift basins including their local melting system.

Strong along-axis segmentation is reported along the conjugate margins of the southern South Atlantic (Clemson et al., 1997; Franke et al., 2007). This segmentation is defined by large transfer zones and corresponding horizontal offsets in the distribution of the SDRs (Fig. 17). Based on distinct along-margin variations in architecture, volume, and width of the SDRs Franke et al. (2007) proposed that this segmentation had considerable influence on the melt supply during rifting and initial seafloor-spreading. An axial-symmetrical small-scale mantle convection system may have developed in localized zones of lithospheric thinning with the transfer zones having acted as rift propagation barriers. Breakup by a successive northward unzipping of rift zones with a triangle-shaped opening of individual margin segments is expected to result in differential stretching along strike of the margin. In such a scissor-like opening model decreasing extension rates toward the north along each individual margin segment result in decreasing volumes of melts. Towards the transfer zones the supply of melt decreases to close to zero while at the other side of the structural discontinuity melting occurs at maximum volumes. This model implies that the melts are derived from below each individual margin segment, similar to the melt supply to newly formed oceanic crust. These melts are from individual sources within each mid-ocean ridge segment as suggested by e.g. results from dense sampling on the highly segmented East Pacific Rise (Salters, 2012). Further, the coincidence of change in source composition at ridge discontinuities indicates that there is little melt transport across a transform fault plane.

5.5 Rift - hot-spot interaction: Top-down control

The findings from three different rifted areas argue for much more top-down control on the magmatism than previously thought. It is proposed here that mode of rifting and the magnitude and timing of volcanism are controlled predominantly by relatively shallow processes (i.e. passive or plate driven) rather than by active, or plume-driven rifting.

In the Laptev Sea region, a close spatial relationship of a rift with a hot-spot did not result in volcanic rifting. Similarly rifting of India from the Seychelles was characterized by modest magmatism despite the close spatial relationship with the Deccan flood basalt province (Armitage et al., 2010; Collier et al., 2009). Therefore there is no unequivocal link between an onshore flood basalt province, indicating the presence of a hot-spot and the volume of magmatism during rifting.

The opening of the South Atlantic was unlikely triggered by the Tristan da Cunha hot-spot. First, there is no spatial relationship. The South Atlantic started opening at its southernmost point, close to the present Falkland-Agulhas Fracture Zone (FAFZ; Fig. 12). The (later) hot-spot was centered more than 2.000 km further north. Second, the timing is not appropriate.

The vast majority of the Etendeka and Paraná flood basalts were emplaced when there was already ongoing seafloor spreading in the south. Thus, the hot-spot came in when rifting had ceased in the South. It can be argued that the plume head was already situated below the rift without major expulsions reaching the surface. But the sharp transition from magma-poor to volcanic rifting as observed at the southern Argentine margin (Franke et al., 2010) and at the South African margin (Fig. 12) argues against a deep mantle origin for the rift-related magmatism. A plume rising from the deep mantle is expected to generate a smooth transition from magma starved to volcanic rifting over a few hundreds of kilometers rather than over a few 10^{th} of kilometers.

In the South China Sea, the Hainan Plume in the South China Sea developed late, about 10 Ma after the cessation of seafloor-spreading. The termination of seafloor-spreading may in fact offer the explanation for the presence of this "plume". In the South China Sea seafloor-spreading ceased at about 20 Myr ago, most likely because of the collision of the southern South China Sea margin with Luzon, the Philippines. It may be speculated that a well established mantle convection system, delivering melts for the production of oceanic crust keeps going after the spreading suddenly got stuck. The melts will find other ways to the surface rather than along the continuous mid-oceanic ridge and this may result in the observed volcanic cones, seamounts and volcanic flows. The position of the Hainan Plume, being centered beneath the extinct spreading ridge may imply that the hot-spot originated from such a setting. The developing hot-spot in this view did cause by itself further decompression of the underlying asthenosphere and consequently more extensive partial melting and melt segregation at progressively deeper levels (Ziegler and Cloetingh, 2004).

Could we assume a similar process for the formation of the Tristan da Cunha hot-spot? Clearly seafloor-spreading was delayed across the southern to the central segments of the South Atlantic. The Brazil-Angola margins of the central segment are extremely stretched, a fact that highlights a much longer rift phase affecting this region before breakup. Rift propagation was delayed, possibly by the presence of more rigid Gondwana-core basement.

The concept of rift propagation barriers which are suggested to enhance the supply of melt from decompressional melting at the opposite side of the structural discontinuity thus is in accordance with the position of flood basalts in the Etendeka and Paraná area. However, we would have to assume that this extension-induced hot-spot had grown downwards. Thereby the concept would be in accordance time-progressive evolution of the "plume tail" expression Walvis Ridge - Rio Grande Rise.

Such concept may be applicable to other areas, as many hot-spots are apparently located at positions where the rift could not propagate straight forward, as e.g. at triple junctions. An intrinsic relationship between mantle plumes and triple junctions was already proposed by Burke and Dewey (1973) for 45 selected junctions. Such a link may in fact exist, but, in contrary to this study it is speculated here that not the hot-spot did generate the junctions but the hot-spot may have developed at a position where rift-propagation was hindered.

Passive continental margins are so diverse that the deduction of concepts and generalized models is not straight forward. Further research will help in better understanding to what degree the volume of rift-related magmatism depends on the pre-rift configuration and the rift history and to what amount elevated mantle temperatures are necessary to explain the origin of volcanic margins.

Acknowledgements

Thanks are due to Gwen Péron-Pivindic, NGU, Trondheim who invited the author to present this topic at the annual EGU meeting in Vienna in 2012. The ideas discussed here, however, had a much longer evolution. First of all I want to thank Karl Hinz for having given me the chance to start my career working on the Laptev Sea data, and for continuous support throughout the years. Colleagues from VSEGEI, St. Petersburg made the expedition to the New Siberian Islands in 2011 possible and I want to thank Pjotr Sobolev, Nicolai Sobelev and Tatiana Tolmacheva on behalf of all others. Dimitri Chizov, Vladimir Verzhbitskiy and Benoit Mouly are thanked for fruitful discussions on the Laptev Sea geology. The perspective on interpreting a breakup unconformity in the Laptev Rift was initially developed by Benoit Mouly. Thorough discussions on the evolution of the South China Sea with Manuel Pubellier, Florian Meresse and Dimitri Savva from the ENS, Paris, Mario Aurelio from the University of the Philippines, Manila, Weiwei Ding from the Second Institute of Oceanography, Hangzhou, as well as with Jean-Luc Auxietre and Benoit Mouly from TOTAL, Paris are acknowledged. Stefan Ladage, Michael Schnabel and Bernd Schreckenberger from BGR, Hannover and the SAMPLE coordinator Peter Bunge on behalf of all participants and the reviewers of that DFG project are thanked for the stimulating discussions on the South Atlantic. Finally, Lutz Reinhard, Christoph Gaedicke and Rüdiger Lutz from BGR, Hannover are thanked for proof-reading the manuscript. This manuscript further benefited from the thoughtful and constructive reviews of Sergey Drachev and an anonymous reviewer.

This is a contribution to project FR 2119/2-2 funded by the Deutsche Forschungsgemeinschaft (German Research Foundation) within the priority program SAMPLE.

FIGURES

Figure 1: Schematic sketch of the end-member extremes of passive continental margins. Top: The magma-poor margin is defined by a wide area of highly attenuated continental crust where the upper crust is deformed by deep-reaching listric faults that may sole out on a common detachment surface, the proximal margin. In the distal margin the listric faults may cut across the entire crust leading to a detachment at the Mohorovičić (MOHO) discontinuity. Further seaward extensional allochthones may be situated on exhumed mantle before relatively thin oceanic crust is reached. Bottom: Volcanic rifted margins show a comparably narrow proximal margin with considerable crustal thinning over a short distance, thick wedges of syn-rift volcanic flows manifest in seismic reflection data as seaward dipping reflectors (SDRs), and wide high-velocity (Vp > 7.3 km/s) lower-crust seaboard of the continental rifted margin. The oceanic crust is comparably thick at those margins, especially close to the continent-ocean transition (COT). ROU is the rift-onset unconformity; BU the breakup unconformity.

Figure 2: Schematic cross section, a seismic data example and the tectonic setting illustrating the pre-rift erosion, the rift sedimentation, and the breakup stages. During pre- or syn-rift doming erosion a rift-onset unconformity (ROU) forms, which in seismic data often is recognized as angular unconformity with top-lap truncations of seismic reflectors from below. A syn-rift infill typically shows wedge shaped reflector packages with the thin end of the wedge lying on the hangingwall dip-slope. The seismic section shows two subsequent rift deposits before subsidence did outpace sedimentation, resulting in a different relief. This indicates the time of maximum displacement, the rift climax (Prosser, 1993). At continental breakup, a flexural rebound results in uplift of the rift shoulders. This frequently results in the formation of a breakup unconformity (BU), truncating the wedge-shaped syn-rift sediments in the rift basins from the draped post-rift sediments. At the basins outer margins the BU is expected to form an amalgamation with the rift-onset unconformity.

Figure 3: Polar stereographic projection of the magnetic anomaly map (Gaina et al., 2011) around the New Siberian Islands, which are located between the Laptev Sea and the East Siberian Sea. The highly magnetized De Long volcanic province is indicated by a dashed white circle. A linear band of high magnetization close to the shore is commonly interpreted as Lyakhov-South Anyui suture**.** Solid red lines show the location of example cross sections shown in Figures 6 and 7. Small yellow circles indicate onshore locations shown in Figure 5. Bathymetric contours are shown for every 1000 m.

Figure 4: Hiatuses around the Laptev Sea Rift System summarized from own studies and earlier investigations (Dorofeev et al., 1999; Drachev et al., 1998; Egorov and Surmilova, 2001 ; Kos'ko et al., 1990; Kos'ko and Trufanov, 2002; Kos'ko and Korago, 2009; Kuzmichev et al., 2009). An Eocene to Miocene major hiatus of sedimentation identified during the Arctic Coring Expedition (ACEX) on the Lomonosov Ridge (Backman et al., 2008) was updated to 36 to 18 Million years (Poirier and Hillaire-Marcel, 2011). The stratigraphic position of the breakup unconformity is correlated with magnetic spreading anomalies in the Eurasia Basin.

Figure 5: (A) Successions of Upper Jurassic – Lower Cretaceous siliciclastic sediments of Stolbovoi Island are interpreted as distal turbidites (Kuzmichev et al., 2009). Three main rock types alternate in the sequence: (1) light dominantly medium grained sandstones; (2) dark-grey clayey sandstones and (3) dark-grey to black mudstones. An Early Cretaceous (c. Hauterivian) compressional phase resulted in folding and shearing. Subsequently a late Aptian to Cenozoic extensional phase (Kuzmichev et al., 2009) resulted in normal faulting as shown by the photography.

(B) Up to 5 km thick Upper Devonian rocks are found on Belkhov Island. The succession from the Upper Devonian to the late Early Carboniferous is similar to that of Kotel'nyi Island but deformation degree is higher. On this island, Paleocene sandstones with minor occurrence of brown coal rest unconformably on Paleozoic sediments.

(C) Thick Late Lower Cretaceous basalts resting on Ordovician turbitites on Bennett Island, located within the De Long volcanic province.

Figure 6: Interpretation of an about 700 km long, complete transect across the Laptev Sea Rift System, from the western edge of the Ust' Lena Rift in the southwest onto the Laptev Horst in the northeast. The location of the line is shown in Figure 3. The interpretation is based on as follows: A-B is modified from MAGE Line 87722 (modified from (Drachev et al., 1998)); B-C MCS line *BGR97-04; C-D* MCS line *BGR94-04; D-E* MCS line *BGR94-02.* The BGR seismic data are shown below the interpretation.

The basement (grey) is separated from unspecified pre-rift strata (green) by a distinct reflection band at about 4-6 s (TWT) depth. An early, seismically transparent rift deposit is shown in beige, a subsequent, more reflective rift deposit in orange. The rift-onset unconformity (ROU; green line) shows some evidence for erosional truncations. The breakup unconformity (BU; orange line) seals the wedge-shaped rift deposits that onlap the unconformity below and terminate against the basin-bounding listric normal faults. There is no indication for magmatism across the entire rift basin. Dashed boxes show where the stratigraphy from (A) Stolbovoi Island (Figure 5a) and (B) Belkhov Island (Figure 5b) may be projected.

Figure 7: The upper panel shows a line-drawing interpretation of MCS line BGR93-09, running across the Laptev Shelf and slope into the Eurasia Basin. The interpretation is tentative because the data-quality is at best moderate; however, it can be reliably stated that the margin is magma-poor, because no indications for SDRs are imaged along that line. ROU is the rift-onset unconformity; BU the breakup unconformity. The location of the line is shown in Figure 3.

Figure 8: Topography and bathymetry of the South China Sea region with the location of the basins discussed. The area of highly attenuated continental crust (yellow/light green) exceeds 1.000 km width. Bathymetry contours are shown every 1.000 m. Tentative age of

the oceanic crust (blue) is indicated. Seafloor spreading anomalies (white, dashed lines) and a major fracture zone (white, solid line), separating the eastern subbasin from the SW subbasin of the South China Sea, are shown according to Barckhausen and Roeser (2004). Location of ODP drilling site 1148 is indicated. Red lines show the location of example seismic sections presented in Figure 10.

Figure 9: Hiatuses around the South China Sea summarized from different sources (Cullen, 2010; Franke et al., 2011; Franke et al., 2008a; Fyhn et al., 2009a; Fyhn et al., 2009b; Grötsch and Mercadier, 1999; Hutchison and Vijayan, 2010; Kudrass et al., 1986; Li et al., 2008; Lin et al., 2003; Lüdmann and Wong, 1999; Sales et al., 1997; Schlüter et al., 1996; Shi et al., 2011; Shipboard Scientific Party, 2000; Sun et al., 2009; Taylor and Hayes, 1980, 1983; Zhou et al., 1995). PRMB is the Pearl River Mouth basin, QDNB the Qiongdongnan basin.

Figure 10: The upper panel shows a line-drawing interpretation of MCS line 08 (Hu et al., 2009), running across the northern margin, and line BGR08-104, running across the conjugate NW Palawan margin (Figure 11). The location of the lines is shown in Figure 8. The depth sections in the lower panel are based on a depth conversion (Hu et al., 2009) and on gravity modeling (Franke et al., 2011). The acoustic basement between the Moho and the rift-onset unconformity (ROU) is shown in green, the rift deposit in orange, and post-rift sediments in yellow. The breakup unconformity (BU) seals the wedge-shaped rift deposits that onlap the unconformity below and terminate against the basin-bounding listric normal faults. Post-rift Neogene and/or Quaternary basalts are interpreted along the lines. There is a considerable thinning of the crust towards the continent-ocean transition (COT), but also beneath individual rift basins.

Figure 11: Example seismic section BGR08-104 showing the rift-onset and the breakup unconformities at the southern margin of the South China Sea. The prominent reflection from the deepwater equivalent of shallow-water platform carbonates (Nido) is indicated. The top of these limestones is at Lower Miocene level (c. 22 Ma to c. 17 Ma). The breakup unconformity

is continuous along the deepwater NW Palawan Basin and is interpreted at the shallow shelf at the base of these carbonates (c. 31 Ma). Toplap-truncations below the rift-onset unconformity (ROU) indicate a Late Cretaceous and younger erosional phase before the onset of rifting. The distinction between the volcanic flow unit, the volcanic province, and the rift basin is discussed in Franke et al., (2011). The inferred position of the continent-ocean transition (COT) is indicated.

Figure 12: The southern South Atlantic region with the location of the basins discussed. Magnetic map is from Maus et al. (2009). There is a distinct and conjugate southern termination of the Large Marginal Magnetic Anomaly, also named G-anomaly that corresponds to the seaward dipping reflectors (SDRs). The continental margin between this magnetic anomaly and the Falkland-Agulhas Fracture Zone (FAFZ) is magma-poor. Black lines show the location of example seismic sections presented in Figure 14. The 1.000 m isobaths are shown in grey. Magnetic seafloor spreading anomalies M0 through M7 are tentatively interpreted (Schreckenberger et al., 2002). The inlay shows a reconstruction at about 130 Ma with a 2.000 km diameter of the Tristan da Cunha plume head. Abbreviations: SDRs – seaward dipping reflectors, MOR – mid-oceanic ridge.

Figure 13: Times of hiatuses in the basins around the southern South Atlantic, summarized from different sources (Baldi and Nevistic, 1996; Brown et al., 1995; de Vera et al., 2009; Fryklund et al., 1996; Gerrard and Smith, 1982; Hinz et al., 1999; Juan et al., 1996; Karner et al., 2003; Lawrence et al., 1999; Light et al., 1993b; Maslanyj et al., 1992; McMillan, 2003; Moulin et al., 2005; Otis and Schneidermann, 2000; Richards and Hillier, 2000; Ross et al., 1996; Séranne and Anka, 2005; Sibuet et al., 1984b; Stoakes et al., 1991; Tavella and Wright, 1996).

Figure 14: The MCS lines BGR98-20 and BGR03-16a are considered as conjugate because both are crossing the continental margins close to the southern end of the Large Marginal Magnetic Anomaly. The upper panels show line-drawing interpretations of MCS line BGR98-20, running across the Argentine margin and of line BGR03-16a, running across the South

African margin. The location of the lines is shown in Figure 12. In the lower panels velocity profiles as derived from refraction seismic modeling were modified and projected onto the lines. The Argentina profile is from Schnabel et al. (2008); the South Africa profile is from Hirsch et al. (2009). While the first line was shot close to the MCS line, the latter profile has an offset of about 200 km. Post-rift sediments are shown in blue, pre-rift sediments in light orange, the upper crust in green and the lower crust (Vp > 6.5 km/s) in grey. High-velocity lower crust (Vp > 7.3 km/s) is shown in orange-red. The seaward dipping reflectors (SDRs) cover an area of about 80 km on the western margin, while they spread over about 100 km on the eastern margin. Also the high-velocity lower crust is much more voluminous on the eastern margin.

Figure 15: Sketches illustrating the early evolution of the southern South Atlantic at (A) c. 137 Ma, (B) c. 133 Ma and (C) c. 128 Ma.

(A) Extension coincident with subsequent seafloor spreading following oblique and magma-poor rifting in the southernmost segment initiated in the late Valanginian or early Hauterivian. The newly formed oceanic crust is thinner than usual (Becker et al., 2012). However, likely there was already strong volcanism at the future volcanic rifted margins, which is manifested in the SDRs.

(B) The segment to the north of the transfer zone, defining the transition from magma-poor to volcanic rifting opens at about 133 Ma. At the next transfer zones further north, rifting is interrupted, resulting in heat accumulation in the upper mantle. This enhances convection in the asthenosphere and the subsequent emplacement of multiple SDRs wedges and the emplacement of the Paraná-Etendeka flood basalts between mainly between 134 and 132 Ma. At this stage a magmatic overprint of the southern segment occurred, resulting in the formation of volcanic outer highs and seaward SDRs sequences.

(C) After stepping across the next segment boundary, or transfer zone, seafloor spreading propagated fast to the north, reaching the transfer zone that bounds the southern to the central South Atlantic by Barremian time. Again heat accumulation and enhanced mantle convection is proposed as for margin segment II, resulting in the emplacement of the multiple SDRs wedges in this margin segment.

Figure 16: Sketch in top-view, showing the expected evolution of a rift that evolves in conjunction with a plume head. As the plume head triggers the rift evolution by a circular uplift, the earliest and widest rift is expected close to the plume head and the width of the rift decreases away from the plume. The contrary is observed in the southern South Atlantic: The rift started in the south, at the most distal point from the plume and rifting migrated to close to the plume only when there was already seafloor-spreading in the south, implying a consistently decreasing width of the rift towards the plume.

Figure 17: Conceptual 3D model for the evolution of a breakup unconformity at magma-poor margins. Seafloor spreading at one location coincides with continuing rifting further along-strike the future margins. The area that is rifted may be below sea-level, as in the South China Sea example, while the area with a well developed oceanic spreading system is elevated. The uplift (grey arrows) affects predominantly the proximal margins of the area that is already in the seafloor-spreading stage. A delayed formation of a breakup unconformity is expected in such setting.

References

Armitage, J.J., Collier, J.S., Minshull, T.A., 2010. The importance of rift history for volcanic margin formation. Nature 465, 913-917.

Aslanian, D., Moulin, M., Olivet, J.-L., Unternehr, P., Matias, L., Bache, F., Rabineau, M., Nouzé, H., Klingelheofer, F., Contrucci, I., Labails, C., 2009. Brazilian and African passive margins of the Central Segment of the South Atlantic Ocean: Kinematic constraints. Tectonophysics 468, 98-112.

Austin, J.A., Uchupi, E., 1982. Continental-Oceanic crustal transition of southwest Africa. AAPG Bulletin 66 1328-1347.

Backman, J., Jakobsson, M., Frank, M., Sangiorgi, F., Brinkhuis, H., Stickley, C., O'Regan, M., Løvlie, R., Pälike, H., Spofforth, D., Gattacecca, J., Moran, K., King, J., Heil, C., 2008. Age model and core-seismic integration for the Cenozoic Arctic Coring Expedition sediments from the Lomonosov Ridge. Paleoceanography 23.

Baldi, J.E., Nevistic, V.A., 1996. Cuenca Costa Afuera del Golfo San Jorge, in: Ramos, V.A., Turic, M.A. (Eds.), Geologia y recursos naturales de la plataforma continental Argentina, relatario XIII◦ Congreso Geologico Argentino y III◦ Congreso de Exploracion de Hidrocarboros. Association Geologica Argentina & Inst. Argentino del Petroleo, Buenos Aires, Argentina, pp. 171-192.

Barckhausen, U., Roeser, H.A., 2004. Seafloor spreading anomalies in the South China Sea revisited, in: Clift, P., Kuhnt, W., Wang, P., Hayes, D.E. (Eds.), Continent-Ocean Interactions in the East Asian Marginal Seas. American Geophysical Union, Geophys. Monograph Series, pp. 121-125.

Bauer, K., Neben, S., Schreckenberger, B., Emmermann, R., Hinz, K., Fechner, N., Gohl, K., Schulze, A., Trumbull, R.B., Weber, K., 2000. Deep structure of the Namibia continental margin as derived from integrated geophysical studies. Journal of Geophysical Research 105, 25829-25853.

Becker, K., Franke, D., Schnabel, M., Schreckenberger, B., Heyde, I., Krawczyk, C.M., 2012. The crustal structure of the southern Argentine margin. Geophysical Journal International 189, 1483-1504.

Bengtson, P., Koutsoukos, E.A.M., 1992. Ammonite and foraminiferal dating of the first marine connection between the central and south Atlantic, Geologie Africaine; 1er colloque de Stratigraphie et de paleogeographie des bassins sedimentaires ouest-africains; 2e colloque africain de Micropaleontologie. Bulletin des Centres de Recherches Exploration-Production Elf-Aquitaine Memoir, Libreville, Gabon, p. pp. 403.

Bialas, R.W., Buck, W.R., Qin, R., 2010. How much magma is required to rift a continent? Earth and Planetary Science Letters 292, 68-78.

Blaich, O.A., Faleide, J.I., Tsikalas, F., 2011. Crustal breakup and continent-ocean transition at South Atlantic conjugate margins. J. Geophys. Res. 116, B01402.

Blaich, O.A., Faleide, J.I., Tsikalas, F., Franke, D., León, E., 2009. Crustal-scale architecture and segmentation of the Argentine margin and its conjugate off South Africa. Geophysical Journal International, 1-21.

Boillot, G., Beslier, M.O., Girardeau, J., 1995. Nature, structure and evolution of the ocean continent boundary: the lesson of the West Galicia Margin (Spain), in: Banda, E., Torne, M., Talwani, M. (Eds.), Rifted Ocean-Continent Boundaries. Kluwer, Dordrecht, pp. 219-229.

Boillot, G., Grimaud, S., Mauffret, A., Mougenot, D., Kornprobst, J., Mergoil-Daniel, J., Torrent, G., 1980. Ocean-continent boundary off the Iberian margin: A serpentinite diapir west of the Galicia Bank. Earth and Planetary Science Letters 48, 23-34.

Bond, G.C., Kominz, M.A., Sheridan, R.E., 1995. Continental Terraces and Rises, in: Busby, C.J., Ingersoll, R.V. (Eds.), Tectonics of Sedimentary Basins. Blackwell Science, Cambridge, MA, pp. 149-178.

Braun, J., Beaumont, C., 1989. A physical explanation of the relation between flank uplifts and the breakup unconformity at rifted continental margins. Geology 17, 760-764.

Briais, A., Patriat, P., Tapponier, P., 1993. Updated interpretation of magnetic anomalies and sea floor spreading stages in the South China Sea: implications for the Tertiary tectonics of Southeast Asia. Journal of Geophysical Research 98, 6299 - 6328.

Bronner, A., Sauter, D., Manatschal, G., Peron-Pinvidic, G., Munschy, M., 2011. Magmatic breakup as an explanation for magnetic anomalies at magma-poor rifted margins. Nature Geosci 4, 549-553.

Brown, L.F., Benson, J.M., Brink, G.J., Doherty, S., Jollands, A., Jungslager, E.H.A., Keenan, J.H.G., Muntingh, A., Van Wyk, N.J.S., 1995. Sequence Stratigraphy in Onshore South African Divergent Basins. American Association Petroleum Geologists, Tulsa.

Brozena, J.M., Childers, V.A., Lawver, L.A., Gahagan, L.M., Forsberg, R., Faleide, J.I., Eldholm, O., 2003. New aerogeophysical study of the Eurasia Basin and Lomonosov Ridge: Implications for basin development. Geology 31, 825-828.

Burke, K., Dewey, J.F., 1973. Plume-generated tripple junctions: Key indicators in applying plate tectonics to old rocks. Journal of Geology 81, 406-433.

Campbell, I.H., 2007. Testing the plume theory. Chem. Geol. 241, 153–176.

Clemson, J., Cartwright, J., Booth, J., 1997. Structural segmentation and the influence of basement structure on the Namibian passive margin. Journal of the Geological Society 154, 477-482.

Clemson, J., Cartwright, J., Swart, J., 1999. The Namib rift: A rift system of possible Karoo age, offshore Namibia, in: Cameron, N.R., Bate, R.H., Clure, V.S. (Eds.), The oil and gas habitats of the South Atlantic. Geological Society London Special Publication London, pp. 381-402.

Clift, P., Lee, G.H., Anh Duc, N., Barckhausen, U., Van Long, H., Zhen, S., 2008. Seismic reflection evidence for a Dangerous Grounds miniplate: No extrusion origin for the South China Sea. Tectonics 27, 1-16.

Clift, P., Lin, J., Barckhausen, U., 2002. Evidence of low flexural rigidity and low viscosity lower continental crust during continental break-up in the South China Sea. Marine and Petroleum Geology 19, 951-970.

Clift, P.D., Lin, J., Odp Leg 184 Scientific, P., 2001. Patterns of extension and magmatism along the continent-ocean boundary, South China margin. Geological Society, London, Special Publications 187, 489-510.

Coakley, B.J., Cochran, J.R., 1998. Gravity evidence of very thin crust at the Gakkel Ridge (Arctic Ocean). Earth and Planetary Science Letters 162, 81-95.

Coffin, M.F., Eldholm, O., 1994. Large igneous provinces: Crustal structure, dimensions, and external consequences. Rev. Geophys. 32, 1-36.

Collier, J.S., Minshull, T.A., Hammond, J.O.S., Whitmarsh, R.B., Kendall, J.M., Sansom, V., Lane, C.I., Rumpker, G., 2009. Factors influencing magmatism during continental breakup: New insights from a wide-angle seismic experiment across the conjugate Seychelles-Indian margins. J. Geophys. Res. 114.

Contreras, J., Zühlke, R., Bowman, S., Bechstädt, T., 2010. Seismic stratigraphy and subsidence analysis of the southern Brazilian margin (Campos, Santos and Pelotas basins). Marine and Petroleum Geology 27, 1952-1980.

Contrucci, I., Matias, L., Moulin, M., Geli, L., Klingelhofer, F., Nouze, H., Aslanian, D., Olivet, J.-L., Rehault, J.-P., Sibuet, J.-C., 2004. Deep structure of the West African continental margin (Congo, Zaïre, Angola), between 5°S and 8°S, from reflectio n/refraction seismics and gravity data. Geophysical Journal International 158, 529-553.

Corner, B., Cartwright, J., Swart, R., 2002. Volcanic passive margin of Namibia: A potential fields perspective, in: Menzies, M.A., Klemperer, S.L., Ebinger, C.J., Baker, J. (Eds.), Volcanic Rifted Margins. Geological Society of America, Boulder, Colorado, pp. 203-220.

Courtillot, V., Davaille, A., Besse, J., Stock, J., 2003. Three distinct types of hotspots in the Earth's mantle. Earth and Planetary Science Letters 205, 295-308.

Cramer, B., Franke, D., 2005. Indications for an active petroleum system in the Laptev Sea, NE Siberia. Journal of Petroleum Geology 28, 1-15.

Cullen, A., Reemst, P., Henstra, G., Gozzard, S., Ray, A., 2010. Rifting of the South China Sea: new perspectives. Petroleum Geoscience 16, 273-282.

Cullen, A.B., 2010. Transverse segmentation of the Baram-Balabac Basin, NW Borneo: refining the model of Borneo's tectonic evolution. Petroleum Geoscience 16, 3-29.

de Vera, J., Granado, P., McClay, K., 2009. Structural evolution of the Orange Basin gravity-driven system, offshore Namibia. Marine and Petroleum Geology In Press, Accepted Manuscript.

Ding, W., Franke, D., Li, J., Steuer, S., 2012. Seismic stratigraphy and tectonic structure from a composite multi-channel seismic profile across the entire Dangerous Grounds, South China Sea. Tectonophysics. DOI: 10.1016/j.tecto.2012.09.026.

Dorofeev, V.K., Blagoveshchensky, M.G., Smirnov, A.N., Ushakov, V.I., 1999. New Siberian Island. Geological structure and metallgeny. VNIIOkeangeologia.

Doust, H., Sumner, H.S., 2007. Petroleum systems in rift basins a collective approach inSoutheast Asian basins. Petroleum Geoscience 13, 127-144.

Drachev, S.S., 2011. Chapter 25 Tectonic setting, structure and petroleum geology of the Siberian Arctic offshore sedimentary basins. Geological Society, London, Memoirs 35, 369-394.

Drachev, S., Saunders, A.D., 2006. The Early Cretaceous Arctic Lip: Its geodynamic setting and implications for Canada Basin opening, in: Scott, R.A., Thurston, D.K. (Eds.), Proceedings of the Fourth International Conference on Arctic Margins ICAM IV. US Department of the Interior, pp. 216-223.

Drachev, S.S., Johnson, G.L., Laxon, S.W., Mcadoo, D.C., Kassens, H., 1999. Main structural elements of Eastern Russian Arctic continental margin derived from satellite gravity and multichannel seismic reflection data, in: Kassens, H., Bauch, H.A., Dmitrenko, I.A., Eicken, H., Hubberten, H.-W., Melles, M., Thiede, J., Timokhov, L.A. (Eds.), Land-Ocean Systems in the Siberian Arctic: Dynamics and History. Springer, pp. 667-692.

Drachev, S.S., Savostin, L.A., Groshev, V.G., Bruni, I.E., 1998. Structure and geology of the continental shelf of the Laptev Sea, Eastern Russian Arctic. Tectonophysics 298, 357-393.

Dragoi-Stavar, D., Hall, S., 2009. Gravity modeling of the ocean-continent transition along the South Atlantic margins. J. Geophys. Res. 114.

Duncan, R.A., Larsen, H.C., Allan, J.F., 1996. Proc. ODP, Init. Repts., 163: College Station, TX (Ocean Drilling Program), p. 279.

Eagles, G., 2007. New angles on South Atlantic opening. Geophysical Journal International 168, 353-361.

Ebbing, J., Lundin, E.R., Olesen, O., Hansen, K., 2006. The mid-Norwegian margin: A discussion of crustal lineaments, mafic intrusions, and remnants of the Caledonian root by 3D density modelling and structural interpretation. Geological Society of London Journal 163, 47-59.

Edwards, P.B., 1992. Structural evolution of the western Pearl River Mouth Basin, in: Watkins, J.S., Feng, Z., Mcmillen, K.J. (Eds.), Geology and Geophysics of Continental Margins. American Association of Petroleum Geologists, pp. 43-52.

Egorov, A.Y., Surmilova, E.P., 2001 State Geological Map of the Russian Federation, Scale 1:1 000 000, Quadrangle S-50-52, Bykovsky, Explanatory notes, 189 pp. (in Russian). VSEGEI Saint-Petersburg.

Eldholm, O., Thiede, J., Taylor, B., 1987. Proc. ODP, Sci. Results. College Station, TX (Ocean Drilling Program).

Eldholm, O., Thiede, J., Taylor, E., 1989. Evolution of the Vøring Volcanic Margin. Proceedings of the Ocean Drilling Program, Scientific Results 104, 1033-1065.

Falvey, D.A., 1974. The development of continental margins in plate tectonic theory. Australian Petroleum Exploration Association Journal 14, 95-107.

Fernàndez, M., Afonso, J.C., Ranalli, G., 2010. The deep lithospheric structure of the Namibian volcanic margin. Tectonophysics In Press, Accepted Manuscript.

Flower, M.F.J., Zhang, M., Chen, C.-Y., Tu, K., Xie, G., 1992. Magmatism in the South China Basin: 2. Post-spreading Quaternary basalts from Hainan Island, south China. Chemical Geology 97, 65-87.

Foulger, G.R., 2005. Mantle plumes: Why the current skepticism? Chinese Science Bulletin 50 1555-1560.

Foulger, G.R., Natland, J.H., 2003. Is “Hotspot”Volcanism a Consequence of Plate Tectonics? Science 300, 921-922.

Franke, D., Barckhausen, U., Baristeas, N., Engels, M., Ladage, S., Lutz, R., Montano, J., Pellejera, N., Ramos, E.G., Schnabel, M., 2011. The continent-ocean transition at the southeastern margin of the South China Sea. Marine and Petroleum Geology 28, 1187-1204.

Franke, D., Barckhausen, U., Heyde, I., Tingay, M., Ramli, N., 2008a. Seismic images of a collision zone offshore NW Sabah/Borneo. Marine and Petroleum Geology 25, 606-624.

Franke, D., Hinz, K., 2005. The structural style of sedimentary basins on the shelves of the Laptev Sea and the western East Siberian Sea, Siberian Arctic. Journal of Petroleum Geology 28, 269-286.

Franke, D., Hinz, K., 2009. Geology of the shelves surrounding the New Siberian Islands, Russian Arctic., in: D. B. Stone, K.F., P. W. Layer, E. L. Miller, A. V. Prokopiev, J. Toro (Ed.), Geology, geophysics and tectonics of Northeastern Russia: a tribute to Leonid Parfenov. Stephan Mueller Spec. Publ. Ser., pp. 35-44.

Franke, D., Hinz, K., Oncken, O., 2001. The Laptev Sea Rift. Marine and Petroleum Geology 18, 1083-1127.

Franke, D., Krüger, F., Klinge, K.D., 2000. Tectonics of the Laptev Sea - Moma 'Rift' region: Investigation with seismologic broadbanddata. Journal of Seismology 4, 99-116.

Franke, D., Ladage, S., Schnabel, M., Schreckenberger, B., Reichert, C., Hinz, K., Paterlini, M., de Abelleyra, J., Siciliano, M., 2010. Birth of a volcanic margin off Argentina, South Atlantic. Geochem. Geophys. Geosyst. 11, Q0AB04.

Franke, D., Neben, S., Ladage, S., Schreckenberger, B., Hinz, K., 2007. Margin segmentation and volcano-tectonic architecture along the volcanic margin off Argentina/Uruguay, South Atlantic. Marine Geology 244, 46-67.

Franke, D., Neben, S., Schreckenberger, B., Schulze, A., Stiller, M., Krawczyk, C.M., 2006. Crustal structure across the Colorado Basin, offshore Argentina. Geophysical Journal International 165, 850-864.

Franke, D., Reichert, C., Damm, V., Piepjohn, K., 2008b. The South Anyui suture, Northeast Arctic Russia, revealed by offshore seismic data. Norwegian Journal of Geology 88, 189-200.

Fryklund, B., Marshal, A., Stevens, J., 1996. Cuenca del Colorado, in: Ramos, V.A., Turic, M.A. (Eds.), Geologia y recursos naturales de la plataforma continental Argentina, relatario XIII◦ Congreso Geologico Argentino y III◦ Congreso de Exploracion de Hidrocarboros. Association Geologica Argentina & Inst. Argentino del Petroleo, Buenos Aires, Argentina, pp. 135-158.

Funck, T., Hopper, J.R., Larsen, H.C., Louden, K.E., Tucholke, B.E., Holbrook, W.S., 2003. Crustal structure of the ocean-continent transition at Flemish Cap: Seismic refraction results. Journal of Geophysical Research 108, 2531.

Fyhn, M.B.W., Boldreel, L.O., Nielsen, L.H., 2009a. Geological development of the Central and South Vietnamese margin: Implications for the establishment of the South China Sea, Indochinese escape tectonics and Cenozoic volcanism. Tectonophysics 478, 184-214.

Fyhn, M.B.W., Nielsen, L.H., Boldreel, L.O., Thang, L.D., Bojesen-Koefoed, J., Petersen, H.I., Huyen, N.T., Duc, N.A., Dau, N.T., Mathiesen, A., Reid, I., Huong, D.T., Tuan, H.A., Hien, L.V., Nytoft, H.P., Abatzis, I., 2009b. Geological evolution, regional perspectives and hydrocarbon potential of the northwest Phu Khanh Basin, offshore Central Vietnam. Marine and Petroleum Geology 26, 1-24.

Gaina, C., Roest, W.R., Muller, R.D., 2002. Late Cretaceous-Cenozoic deformation of northeast Asia. Earth and Planetary Science Letters 197, 273-286.

Gaina, C., Werner, S.C., Saltus, R., Maus, S., GROUP, t.C.-G., 2011. Chapter 3 Circum-Arctic mapping project: new magnetic and gravity anomaly maps of the Arctic. Geological Society, London, Memoirs 35, 39-48.

Gernigon, L., Lucazeau, F., Brigaud, F., Ringenbach, J.-C., Planke, S., Le Gall, B., 2006. A moderate melting model for the Voring margin (Norway) based on structural observations and a thermo-kinematical modelling: Implication for the meaning of the lower crustal bodies. Tectonophysics 412, 255-278.

Gerrard, I., Smith, G.C., 1982. Post paleozoic succession and structure of the Southwestern African continental margin, in: J.S.Watkins, C.L.Drake (Eds.), Studies in Continental Margin Geology Am. Assoc. Petrol. Geol. Mem., pp. 49-74.

Gladczenko, T.P., Hinz, K., Eldholm, O., Meyer, H., Neben, S., Skogseid, J., 1997. South Atlantic volcanic margins. Journal of the Geological Society 154, 465-470.

Gladczenko, T.P., Skogseid, J., Eldhom, O., 1998. Namibia volcanic margin. Marine Geophysical Researches 20, 313-341.

Glebovsky, V.Y., Kaminsky, V.D., Minakov, A.N., Merkur'ev, S.A., Childers, V.A., Brozena, J.M., 2006. Formation of the Eurasia in the Arctic ocean as inferred from geohistorical analysis of the anomalous magnetic field. Geotectonics 40, 263-281.

Glen, J.M.G., Renne, P.R., Milner, S.C., Coe, R.S., 1997. Magma flow inferred from anisotropy of magnetic susceptibility in the coastal Paraná-Etendeka igneous province: Evidence for rifting before flood volcanism. Geology 25, 1131-1134.

Gradstein, F.M., Ogg, J.G., Smith, A.G., 2004. A Geologic Time Scale 2004 Cambridge University Press, Cambridge.

Grassmann, S., Franke, D., Neben, S., Schnabel, M., Damm, V., 2011. Maturity Modelling of the Deepwater Continental Margin, offshore Argentina. Z. dt. Ges. Geowiss. (ZDGG) 162, 79-89.

Grötsch, J., Mercadier, C., 1999. Integrated 3-D Reservoir Modeling Based on 3-D Seismic: The Tertiary Malampaya and Camago Buildups, Offshore Palawan, Philippines. AAPG Bulletin 83, 1703-1728.

Gruetzner, J., Uenzelmann-Neben, G., Franke, D., 2012. Variations in sediment transport at the central Argentine continental margin during the Cenozoic. Geochem. Geophys. Geosyst. 13, Q10003.

Guong, Z., Jin, Q., Qiu, Z., Wang, S., Meng, J., 1989. Geology, tectonics and evolution of the Pearl River Mouth Basin. Chinese sedimentary basins, 181-196.

Hall, R., Morley, C.K., 2004. Sundaland Basins, Continent–Ocean Interactions Within East Asian Marginal Seas. American Geophysical Union, Geophyscial Monograph Series, pp. 55-85.

Harry, D.L., Sawyer, D.S., 1992. Basaltic volcanism, mantle plumes, and the mechanics of rifting: The Paraná flood basalt province of South America. Geology 20, 207-210.

Hawkesworth, C.J., Gallagher, K., Kelly, S., Mantovani, M.S.M., Peate, D.W., Regelows, R., Rogers, N.W., 1992. Paraná magmatism and the opening of the South Atlantic, in: Storey, B.C., Alabaster, T., Pankhurst, R.J. (Eds.), Magmatism and the Causes of Continental Break-up. Geol. Soc. London, Spec. Publ. , pp. 221-240.

Hawkesworth, C.J., Kelley, S., Turner, S., le Roex, A., Storey, B., 1999. Mantle processes during Gondwana break-up and dispersal. Journal of African Earth Sciences 28, 239-261.

Hayes, D.E., Nissen, S.S., 2005. The South China sea margins: Implications for rifting contrasts. Earth and Planetary Science Letters 237, 601-616.

Hinz, K., 1981. A hypothesis on terrestrial catastrophes: wedges of very thick oceanward dipping layers beneath passive continental margins—their origin and paleoenvironmental significance. Geologisches Jahrbuch Reihe E, 3-28.

Hinz, K., Neben, S., Schreckenberger, B., Roeser, H.A., Block, M., Souza, K.G.d., Meyer, H., 1999. The Argentine continental margin north of 48°S: sedimentary successions, volcanic activity during breakup. Marine and Petroleum Geology 16, 1-25.

Hinz, K., Schlüter, H.U., 1985. Geology of the dangerous grounds, South China Sea, and the continental margin of southwest Palawan: Results of Sonne cruises SO-23 and SO-27. Energy 10, 297-315.

Hirsch, K.K., Bauer, K., Scheck-Wenderoth, M., 2009. Deep structure of the western South African passive margin -- Results of a combined approach of seismic, gravity and isostatic investigations. Tectonophysics 470, 57-70.

Hoolbrook, W.S., Mooney, W.D., Christiansen, N.I., 1982. The seismic velocity structure of the deep continental crust, in: Fountain, D.M., Arculus, R., Kay, R. (Eds.), Continental Lower Crust. Elsevier Amsterdam, pp. 1-43.

Hopper, J.R., Funck, T., Tucholke, B.E., 2007. Structure of the Flemish Cap margin, Newfoundland: insights into mantle and crustal processes during continental breakup, in: Karner, G., Manatschal, G., Pinheiro, L.D. (Eds.), Imaging, Mapping and Modelling Continental Lithosphere Extension and Breakup. Geological Society of London Special Publication, London, pp. 47-61.

Hsu, S.-K., Yeh, Y.-c., Doo, W.-B., Tsai, C.-H., 2004. New Bathymetry and Magnetic Lineations Identifications in the Northernmost South China Sea and their Tectonic Implications. Marine Geophysical Researches 25, 29-44.

Hu, D., Zhou, D., Wu, X., He, M., Pang, X., Wang, Y., 2009. Crustal structure and extension from slope to deepsea basin in the northern South China Sea. Journal of Earth Science 20, 27-37.

Hutchison, C.S., 2004. Marginal basin evolution: the southern South China Sea. Marine and Petroleum Geology 21, 1129-1148.

Hutchison, C.S., Vijayan, V.R., 2010. What are the Spratly Islands? Journal of Asian Earth Sciences 39, 371-385.

Ingram, G.M., Chisholm, T.J., Grant, C.J., Hedlund, C.A., Stuart-Smith, P., Teasdale, J., 2004. Deepwater North West Borneo: hydrocarbon accumulation in an active fold and thrust belt. Marine and Petroleum Geology 21, 879-887.

Jackson, M.P.A., Cramez, C., Fonck, J.-M., 2000. Role of subaerial volcanic rocks and mantle plumes in creation of South Atlantic margins: implications for salt tectonics and source rocks. Marine and Petroleum Geology 17, 477-498.

Jokat, W., Boebel, T., König, M., Meyer, U., 2003. Timing and geometry of early Gondwana breakup. Journal of Geophysical Research 108.

Juan, R.d.C., De Jager, J., Russell, J., Gebhard, I., 1996. Flanco norte de la cuenca del Colorado, in: Ramos, V.A., Turic, M.A. (Eds.), Geologia y recursos naturales de la plataforma continental Argentina, relatario XIII° Congreso Geologico Argentino y III° Congreso de Exploracion de Hidrocarboros. Association Geologica Argentina & Inst. Argentino del Petroleo, Buenos Aires, Argentina, pp. 117-134.

Karner, G.D., Driscoll, N.W., 2000. Style, timing and distribution of tectonic deformation across the Exmouth Plateau, northwest Australia, determined from stratal architecture and quantitative basin modelling. Geol. Soc. Spec. Publ. 164, 271-311.

Karner, G.D., Driscoll, N.W., Barker, D.H.N., 2003. Syn-rift regional subsidence across the West African continental margin: the role of lower plate ductile extension. Geological Society, London, Special Publications 207, 105-129.

Keeley, M.L., Light, M.P.R., 1993. Basin evolution and prospectivity of the Argentine continental margin. Journal of Petroleum Geology 16, 451-464.

Keen, C.E., Potter, D.P., 1995a. Formation and evolution of the Nova Scotian rifted margin: Evidence from deep seismic reflection data. Tectonics 14, 918-932.

Keen, C.E., Potter, D.P., 1995b. The transition from a volcanic to a nonvolcanic rifted margin off eastern Canada. Tectonics 14, 359-371.

Kelemen, P.B., Holbrook, W.S., 1995. Origin of thick, high-velocity igneous crust along the U.S. East Coast Margin. J. Geophys. Res. 100, 10077-10094.
Kido, Y., Suyehiro, K., Kinoshita, H., 2001. Rifting to Spreading Process along the Northern Continental Margin of the South China Sea. Marine Geophysical Researches 22, 1-15.
King, S.D., Anderson, D.L., 1998. Edge-driven convection. Earth and Planetary Science Letters 160, 289-296.
Korenaga, J., Kelemen, P.B., Holbrook, W.S., 2002. Methods for resolving the origin of large igneous provinces from crustal seismology. Journal of Geophysical Research 107, 2178.
Kos'ko, M.K., Lopatin, B.G., Ganelin, V.G., 1990. Major geological features of the islands of the East Siberian and Chukchi Seas and the northern coast of Chukotka. Marine Geology 93, 349-367.
Kos'ko, M.K., Trufanov, G.V., 2002. Middle Cretaceous to Eopleistocene Sequences on the New Siberian Islands: an approach to interpret offshore seismic. Marine and Petroleum Geology 19, 901-919.
Kos’ko, M., Korago, E., 2009. Review of geology of the New Siberian Islands between the Laptev and the East Siberian Seas, North East Russia, in: Stone, D.B., Fujita, K., Layer, P.W., Miller, E.L., Prokopiev, A.V., Toro, J. (Eds.), Stephan Mueller Special Publication Series - Geology, geophysics and tectonics of Northeastern Russia: a tribute to Leonid Parfenov, pp. 45-64.
Kudrass, H.R., Wiedicke, M., Cepek, P., Kreuzer, H., Müller, P., 1986. Mesozoic and Cainozoic rocks dredged from the South China Sea (Reed Bank area) and Sulu Sea and their significance for plate-tectonic reconstructions. Marine and Petroleum Geology 3, 19-30.
Kusznir, N.J., Marsden, G., Egan, S.S., 1991. A flexural-cantilever simple-shear/pure-shear model of continental lithosphere extension: applications to the Jeanne d’Arc Basin, Grand Banks and Viking Graben, North Sea. Geological Society, London, Special Publications 56, 41-60.
Kuzmichev, A.B., 2009. Where does the South Anyui suture go in the New Siberian islands and Laptev Sea?: Implications for the Amerasia basin origin. Tectonophysics 463, 86-108.
Kuzmichev, A.B., Zakharov, V.A., Danukalova, M.K., 2009. New data on the stratigraphy and depositional environment for Upper Jurassic and Lower Cretaceous deposits of the Stolbovoi Island (New Siberian Islands). Stratigraphy and Geological Correlation 17, 396-414.
Larsen, H.C., Saunders, A.D., 1998. Tectonism and volcanism at the southeast Greenland rifted margin: A record of plume impact and later continental rupture, Proc. Ocean Drill. Program Sci. Results. ODP, pp. 503-534.
Larsen, H.C., Saunders, A.D., Clift, P.D., 1994. Proc. ODP, Init. Repts, 152: College Station, TX (Ocean Drilling Program), p. 977.
Lawrence, S.R., Johnson, M., Tubb, S.R., Marshallsea, S.J., 1999. Tectono-stratigraphic evolution of the North Falkland region, in: Cameron, N.R., Bate, R.H., Clure, V.S. (Eds.), The oil and gas habitats of the South Atlantic. Spec. Publ. Geol. Soc. , London, pp. 409-424.
Layer, P.W., Newberry, R., Fujita, K., Parfenov, L., Trunilina, V., Bakharev, A., 2001. Tectonic setting of the plutonic belts of Yakutia, northeast Russia, based on 40Ar/39Ar geochronology and trace element geochemistry. Geology 29, 167-170.
Lee, G.H., Watkins, J.S., 1998. Seismic Sequence Stratigraphy and Hydrocarbon Potential of the Phu Khanh Basin, Offshore Central Vietnam, South China Sea. AAPG Bulletin 82 1711 - 1735.
Lei, J., Zhao, D., Steinberger, B., Wu, B., Shen, F., Li, Z., 2009. New seismic constraints on the upper mantle structure of the Hainan plume. Physics of the Earth and Planetary Interiors 173, 33-50.
Li, C.-F., Zhou, Z., Hao, H., Chen, H., Wang, J., Chen, B., Wu, J., 2008. Late Mesozoic tectonic structure and evolution along the present-day northeastern South China Sea continental margin. Journal of Asian Earth Sciences 31, 546-561.
Light, M.P.R., Keeley, M.L., Maslanyi, M.P., Urien, C.M., 1993a. The tectono-stratigraphic development of Patagonia, and its relevance to hydrocarbon exploration. Journal of Petroleum Geology 16, 465-482.
Light, M.P.R., Maslanyi, M.P., Greenwood, R.J., Banks, N.L., 1993b. Seismic sequence stratigraphy and tectonics offshore Namibia, in: Williams, G.D., Dobb, A. (Eds.), Geological Society Special Publication: Tectonics and seismic sequence stratigraphy. Geological Society, London, pp. 163-191.
Lin, A.T., Watts, A.B., Hesselbo, S.P., 2003. Cenozoic stratigraphy and subsidence history of the South China Sea margin in the Taiwan region. Basin Research 15, 453-478.
Lüdmann, T., Wong, H.K., 1999. Neotectonic regime on the passive continental margin of the northern South China Sea. Tectonophysics 311, 113-138.
Lundin, E.R., Doré, A.G., 2011. Hyperextension, serpentinization, and weakening: A new paradigm for rifted margin compressional deformation. Geology 39, 347-350.
Macdonald, D., Gomez-Perez, I., Franzese, J., Spalletti, L., Lawver, L., Gahagan, L., Dalziel, I., Thomas, C., Trewin, N., Hole, M., Paton, D., 2003. Mesozoic break-up of SW Gondwana:

implications for regional hydrocarbon potential of the southern South Atlantic. Marine and Petroleum Geology 20, 287-308.

Manatschal, G., Bernoulli, D., 1999. Architecture and tectonic evolution of nonvolcanic margins: Present day Galicia and ancient Adria. Tectonics 18, 1099-1119.

Martins-Neto, M.A., Catuneanu, O., 2010. Rift sequence stratigraphy. Marine and Petroleum Geology 27, 247-253.

Maslanyj, M.P., Light, M.P.R., Greenwood, R.J., Banks, N.L., 1992. Extension tectonics offshore Namibia and evidence for passive rifting in the South Atlantic. Marine and Petroleum Geology 9, 590-601.

Maus, S., Barckhausen, U., Berkenbosch, H., Bournas, N., Brozena, J., Childers, V., Dostaler, F., Fairhead, J.D., Finn, C., von Frese, R.R.B., Gaina, C., Golynsky, S., Kucks, R., Lühr, H., Milligan, P., Mogren, S., Müller, R.D., Olesen, O., Pilkington, M., Saltus, R., Schreckenberger, B., Thébault, E., Caratori Tontini, F., 2009. EMAG2: A 2–arc min resolution Earth Magnetic Anomaly Grid compiled from satellite, airborne, and marine magnetic measurements. Geochem. Geophys. Geosyst. 10, Q08005.

McMillan, I.K., 2003. Foraminiferally defined biostratigraphic episodes and sedimentation pattern of the cretaceous drift succession (Early Barremian to Late Maastrichian) in seven basins of the South African and Southern Namibian Continental margin., , . South African Journal od Science 99, 537-576.

Menzies, M.A., Klemperer, S.L., Ebinger, C.J., Baker, J., 2002. Characteristics of volcanic rifted margins, in: Menzies, M.A., Klemperer, S.L., Ebinger, C.J., Baker, J. (Eds.), Volcanic Rifted Margins. Geological Society of America Special Paper Boulder, Colorado, pp. 1-14.

Miall, A.D., 2000. Principles of Sedimentary Basin Analysis. Springer, Berlin.

Mohn, G., Manatschal, G., Beltrando, M., Masini, E., Kusznir, N., 2012. Necking of continental crust in magma-poor rifted margins: Evidence from the fossil Alpine Tethys margins. Tectonics 31, TC1012.

Mohriak, W.U., Leroy, S., 2012. Architecture of rifted continental margins and break-up evolution: insights from the South Atlantic, North Atlantic and Red Sea–Gulf of Aden conjugate margins. Geological Society, London, Special Publications 369.

Mohriak, W., Nemčok, M., Enciso, G., 2008. South Atlantic divergent margin evolution: rift-border uplift and salt tectonics in the basins of SE Brazil. Geological Society, London, Special Publications 294, 365-398.

Mohriak, W.U., Hobbs, R., Dewey, J.F., 1990. Basin-forming processes and the deep structure of the Campos Basin, offshore Brazil. Marine and Petroleum Geology 7, 94-100.

Montadert, L., Roberts, D.G., Charpal, O.d., Guennoc, P., 1979. 54. Rifting and Subsidence of the Northern Continental Margin of the Bay of Biscay, in: Montadert, L., Roberts, D.G. (Eds.), Initial Reports of the Deep Sea Drilling Project Volume 48 pp. 1025-1060.

Montelli, R., Nolet, G., Dahlen, F.A., Masters, G., 2006. A catalogue of deep mantle plumes: New results from finite-frequency tomography. Geochem. Geophys. Geosyst. 7, Q11007.

Morgan, W.J., 1971. Convection plumes in the lower mantle. Nature 230, 42-43.

Moulin, M., Aslanian, D., Olivet, J.-L., Contrucci, I., Matias, L., Geli, L., Klingelhoefer, F., Nouze, H., Rehault, J.-P., Unternehr, P., 2005. Geological constraints on the evolution of the Angolan margin based on reflection and refraction seismic data (ZaïAngo project). Geophysical Journal International 162, 793-810.

Moulin, M., Aslanian, D., Unternehr, P., 2009. A new starting point for the South and Equatorial Atlantic Ocean. Earth-Science Reviews 97, 59-95.

Mutter, J.C., Talwani, M., Stoffa, P.L., 1982. Origin of seaward-dipping reflectors in oceanic crust off the Norwegian margin by "subaerial sea-floor spreading". Geology 10, 353-357.

Nikishin, A.M., Ziegler, P.A., Abbott, D., Brunet, M.F., Cloetingh, S., 2002. Permo–Triassic intraplate magmatism and rifting in Eurasia: implications for mantle plumes and mantle dynamics. Tectonophysics 351, 3-39.

Nissen, S.S., Hayes, D.E., Bochu, Y., Weijun, Z., Yongqin, C., Xiaupin, N., 1995. Gravity, heat flow, and seismic constraints on the processes of crustal extension: Northern margin of the South China Sea. Journal of Geophysical Research 100.

Nürnberg, D., Müller, R.D., 1991. The tectonic evolution of the South Atlantic from Late Jurassic to present. Tectonophysics 191, 27-53.

O'Reilly, B.M., Hauser, F., Jacob, A.W.B., Shannon, P.M., 1996. The lithosphere below the Rockall Trough: wide-angle seismic evidence for extensive serpentinisation. Tectonophysics 255, 1-23.

Otis, R.M., Schneidermann, N., 2000. A failed hydrocarbon system - Rawson Basins, Argentina, in: Mello, M.R., Katz, B.J. (Eds.), Petroleum systems of South Atlantic margins : an outgrowth of the

AAPG/ABGP Hedberg Research Symposium, Rio de Janeiro, Brazil, November 16-19, 1997. AAPG Memoir, Tulsa, OK., pp. 417 - 427.
Parfenov, L.M., Badarch, G., Berzin, N.A., Khanchuk, A.I., Kuzmin, M.I., Nokleberg, W.J., Prokopiev, A.V., Ogasawara, M., Yan, H., 2009. Summary of Northeast Asia geodynamics and tectonics, in: Stone, D.B., Fujita, K., Layer, P.W., Miller, E.L., Prokopiev, A.V., Toro, J. (Eds.), Stephan Mueller Special Publication Series - Geology, geophysics and tectonics of Northeastern Russia: a tribute to Leonid Parfenov, pp. 11-33.
Pautot, G., Rangin, C., Briais, A., Wu, J., Han, S., Li, H., Lu, Y., Zhao, J., 1990. The axial ridge of the South China Sea: a seabeam and geophysical survey. Oceanologica Acta 13 129-143.
Peate, D.W., Hawkesworth, C.J., Mantovani, M.S.M., Shukowsky, W., 1990. Mantle plumes and flood-basalt stratigraphy in the Paraná, South America. Geology 18, 1223-1226.
Péron-Pinvidic, G., Manatschal, G., 2009. The final rifting evolution at deep magma-poor passive margins from Iberia-Newfoundland: a new point of view. International Journal of Earth Sciences 98, 1581-1597.
Péron-Pinvidic, G., Manatschal, G., Minshull, T.A., Sawyer, D.S., 2007. Tectonosedimentary evolution of the deep Iberia-Newfoundland margins: Evidence for a complex breakup history. Tectonics 26.
Péron-Pinvidic, G., Shillington, D.J., Tucholke, B.E., 2010. Characterization of sills associated with the U reflection on the Newfoundland margin: evidence for widespread early post-rift magmatism on a magma-poor rifted margin. Geophysical Journal International 182, 113-136.
Poirier, A., Hillaire-Marcel, C., 2011. Improved Os-isotope stratigraphy of the Arctic Ocean. Geophysical Research Letters 38, 1-6.
Prosser, S., 1993. Rift-related linked depositional systems and their seismic expression. Geological Society, London, Special Publications 71, 35-66.
Qiu, X., Ye, S., Wu, S., Shi, X., Zhou, D., Xia, K., Flueh, E.R., 2001. Crustal structure across the Xisha Trough, northwestern South China Sea. Tectonophysics 341, 179-193.
Rabinowitz, P.D., Labrecque, J.L., 1979. The Mesozoic South Atlantic Ocean and evolution of its continental margins. Journal of Geophysical Research 84, 5973-6002.
Rehder, S., Franke, D., 2012. How to Include Ignorance into Hydrocarbon-Resource Assessments? A Case Study applied to the Presence of Source Rock at the Argentine Deep Water Margin. Natural Resources Research 21, 301-309.
Reston, T.J., 2007. The formation of non-volcanic rifted margins by the progressive extension of the lithosphere: the example of the West Iberia margin, in: Karner, G., Manatschal, G., Pinheiro, L.D. (Eds.), Imaging, Mapping and Modelling Continental Lithosphere Extension and Breakup. Geological Society of London Special Publication, London, pp. 77-110.
Richards, M.A., Duncan, R.A., Courtillot, V.E., 1989. Flood Basalts and Hot-Spot Tracks: Plume Heads and Tails. Science 246, 103-107.
Richards, P.C., Fannin, N.G.T., 1997. Geology of the North Falkland Basin. Journal of Petroleum Geology 20, 165-183.
Richards, P.C., Hillier, B.V., 2000. Post-drilling Analysis of the North Falkland Basin — Part 1: Tectono-stratigraphic framework. Journal of Petroleum Geology 23, 253-272.
Roberts, D.G., Backman, J., Morton, A.C., Murray, J.W., Keene, J.B., 1984. Evolution of volcanic rifted margins: Synthesis of Leg 81 results on the west margin of Rockall Plateau, Initial Reports of the Deep Sea Drilling Project 81. Texas A & M University, Ocean Drilling Program, College Station, TX, United States, pp. 883-911.
Roberts, D.G., Bally, A.W., 2012. From rifts to passive margins: A continuum of extension (Chapter 2), in: Roberts, D.G., Bally, A.W. (Eds.), Regional Geology and Tectonics: Phanerozoic Rift Systems and Sedimentary Basins. Elsevier, Amsterdam, pp. 19-31.
Ross, J.G., Pichin, J., Griffin, D.G., Dinkelmann, M.G., Turic, M.A., Nevistic, V.A., 1996. Cuenca de Malvinas Norte, in: Ramos, V.A., Turic, M.A. (Eds.), Geologia y recursos naturales de la plataforma continental Argentina, relatario XIII◦ Congreso Geologico Argentino y III◦ Congreso de Exploracion de Hidrocarboros. Association Geologica Argentina & Inst. Argentino del Petroleo, Buenos Aires, Argentina, pp. 253-271.
Ru, K., Di, Z., Chen, H.-Z., 1994. Basin evolution and hydrocarbon potential of the northern South China Margin, in: Di, Z.e.a. (Ed.), Oceanology of China Seas, pp. 361-372.
Ru, K., Pigott, J.D., 1986. Episodic rifting and subsidence in the South China Sea. AAPG Bulletin 70, 1136-1155.
Rudnick, R.L., Fountain, D.M., 1995. Nature and composition of the continental crust: A lower crustal perspective. Rev. Geophys. 33, 267-309.
Russell, S.M., Whitmarsh, R.B., 2003. Magmatism at the west Iberia non-volcanic rifted continental margin: evidence from analyses of magnetic anomalies. Geophysical Journal International 154, 706-730.

Sales, A.O., Jacobsen, E.C., Morado, J.A.A., Benavidez, J.J., Navarro, F.A., Lim, A.E., 1997. The petroleum potential of deep-water northwestPalawan Block GSEC 66. Journal of Asian Earth Sciences 15, 217-240.
Salters, V., 2012. The effect of variable mantle composition on melt generation and extraction at mid-ocean ridges, EGU General Assembly 2012 Geophysical Research Abstracts EGU2012-6494, Vienna.
Saltus, R.W., Miller, E.L., Gaina, C., Brown, P.J., 2011. Chapter 4 Regional magnetic domains of the Circum-Arctic: a framework for geodynamic interpretation. Geological Society, London, Memoirs 35, 49-60.
Schlüter, H.U., Hinz, K., Block, M., 1996. Tectono-stratigraphic terranes and detachment faulting of the South China Sea and Sulu Sea. Marine Geology 130, 39-51.
Schnabel, M., Franke, D., Engels, M., Hinz, K., Neben, S., Damm, V., Grassmann, S., Pelliza, H., Dos Santos, P.R., 2008. The structure of the lower crust at the Argentine continental margin, South Atlantic at 44°S. Tectonophysics 454, 14-22.
Schreckenberger, B., Hinz, K., Franke, D., Neben, S., Roeser, H.A., 2002. Marine Magnetic Anomalies and the Symmetry of the Conjugated Rifted Margins of the South Atlantic. Eos Trans. AGU, Fall Meet. Suppl. T52C-1217 83.
Sekretov, S.B., 2001. Northwestern margin of the East Siberian Sea, Russian Arctic: seismic stratigraphy, structure of the sedimentary cover and some remarks on the tectonic history. Tectonophysics 339, 353-371.
Sekretov, S.B., 2002. Structure and tectonic evolution of the Southern Eurasia Basin, Arctic Ocean. Tectonophysics 351, 193-243.
Sengör, A.M.C., Burke, K., 1978. Relative Timing of Rifting and Volcanism on Earth and Its Tectonic Implications. Geophysical Research Letters 5, 419-421.
Séranne, M., Anka, Z., 2005. South Atlantic continental margins of Africa: A comparison of the tectonic vs climate interplay on the evolution of equatorial west Africa and SW Africa margins. Journal of African Earth Sciences 43, 283-300.
Shi, X., Kohn, B., Spencer, S., Guo, X., Li, Y., Yang, X., Shi, H., Gleadow, A., 2011. Cenozoic denudation history of southern Hainan Island, South China Sea: Constraints from low temperature thermochronology. Tectonophysics 504, 100-115.
Shipboard Scientific Party, 1987. Introduction, objectives, and principal results: Ocean Drilling Program Leg103, West Galicia margin, in: Boillot G., Winterer E. L., Meyer A. W., et al. (Eds.), Ocean Drill Program Init. Rep. 103, pp. 3-17.
Shipboard Scientific Party, 2000. Leg 184 Summary: Exploring the Asian Monsoon through Drilling in the South China Sea, in: Wang, P., Prell, W., Blum, P. (Eds.), Proc. ODP, Initial Results. IODP, College Station, TX, pp. 1-77.
Sibuet, J.-C., Hay, W.W., Prunier, A., Montadert, L., Hinz, K., Fritsch, J., 1984a. Early evolution of the South Atlantic Ocean: Role of the rifting episode, in: Hay, W.W., Sibuet, J.-C., et al. (Eds.), Initial Reports of the Deep Sea Drilling Project 75, pp. 469-481.
Sibuet, J.-C., Hay, W.W., Prunier, A., Montadert, L., Hinz, K., Fritsch, J., 1984b. The eastern Walvis Ridge and adjacent basins (South Atlantic): Morphology, stratigraphy, and structural evolution in light of th eresults of Legs 40 and 751, in: Hay, W.W., Sibuet, J.-C., et al. (Eds.), Initial Reports of the Deep Sea Drilling Project 75, pp. 483-508.
Sibuet, J.C., Mazé, J.P., Amortila, P., Pichon, X.L., 1987. Physiography and structure of the western Iberian continental margin off Galicia from Sea-Beam and seismic data, in: Boillot, G., Winterer, E.L., Meyer, A.W. (Eds.), Proc. Init. Repts (Part. A) ODP, 103, pp. 77-97.
Simon, K., Huismans, R.S., Beaumont, C., 2009. Dynamical modelling of lithospheric extension and small-scale convection: implications for magmatism during the formation of volcanic rifted margins. Geophysical Journal International 176, 327-350.
Skogseid, J., 2001. Volcanic margins: geodynamic and exploration aspects. Marine and Petroleum Geology 18, 457-461.
Sleep, N.H., 1971. Thermal Effects of the Formation of Atlantic Continental Margins by Continental Break up. Geophysical Journal of the Royal Astronomical Society 24, 325-350.
Sokolov, S.D., Bondarenko, G.Y., Morozov, O.L., Shekhovtsov, V.A., Glotov, S.P., Ganelin, A.V., Kravchenko-Berezhnoy, I.R., 2002. South Anyui suture, northeast Arctic Russia: Facts and problems. Geological Society of America Special Paper 360: Tectonic Evolution of the Bering Shelf-Chukchi Sea-Artic Margin and Adjacent Landmasses 360, 209-224.
Stoakes, F.A., Campbell, C.V., Cass, R., Ucha, N., 1991. Seismic stratigraphic analysis of the Punta del Este Basin, offshore Uruguay, South America. AAPG Bulletin 75, 219-240.
Stollhofen, H., 1999. Karoo Synrift-Sedimentation und ihre tektonische Kontrolle am entstehenden Kontinentalrand Namibias. *Zeitschrift der deutschen geologischen Gesellschaft* 149 (4), 519-632.

Sun, Z., Zhong, Z., Keep, M., Zhou, D., Cai, D., Li, X., Wu, S., Jiang, J., 2009. 3D analogue modeling of the South China Sea: A discussion on breakup pattern. Journal of Asian Earth Sciences 34, 544-556.

Szatmari, P., 2000. Habitat of petroleum along the South Atlantic margins, in: Mello, M.R., Katz, B.J. (Eds.), Petroleum systems of South Atlantic margins. AAPG Memoir pp. 69-75.

Talwani, M., Abreu, V., 2000. Inferences regarding initiation of oceanic crust formation from the U.S. East Coast Margin and Conjugate South Atlantic Margins, in: Mohriak, W., Talwani, M. (Eds.), Atlantic Rifts and Continental Margins. American Geophysical Union, Washington, DC, pp. 211-234.

Tankard, A.J., Uliana, M.A., Welsink, H.J., Ramos, V.A., Turic, M., Franca, A.B., Milani, E.J., Neves, d.B., B.B., E., N., Skarmeta, J., Santa Ana, H., Wiens, F., Cirbian, M., P.O., L., Germs, G.J.B., De Witt, M.J., Machacha, T., Miller, R.M., 1995. Structural and Tectonic Controls of Basin Evolution in Southwestern Gondwana During the Phanerozoic, in: Tankard, A.J., Suárez Soruco, R., Welsink, H.J. (Eds.), Petroleum basins of South America. Am. Assoc. Petrol. Geol. Mem., U.S.A., pp. 5-52.

Tavella, G.F., Wright, C.G., 1996. Cuenca del Salado, in: Ramos, V.A., Turic, M.A. (Eds.), Geologia y recursos naturales de la plataforma continental Argentina, relatario XIII° Congreso Geologico Argentino y III° Congreso de Exploracion de Hidroca rboros. Association Geologica Argentina & Inst. Argentino del Petroleo, Buenos Aires, Argentina, pp. 95-116.

Taylor, B., Hayes, D.E., 1980. The tectonic evolution of the South China Basin, in: Hayes, D.E. (Ed.), The Tectonic and Geologic Evolution of Southeast Asian Seas and Islands, Part 1. Am. Geophys. Union Geophys. Monogr., pp. 89-104.

Taylor, B., Hayes, D.E., 1983. Origin and history of the South China Sea Basin, in: Hayes, D.E. (Ed.), The Tectonic and Geologic Evolution of Southeast Asian Seas and Islands. AGU, Washington, DC, pp. 23-56.

Thies, K., Mansor, A., Hamdon, M., Bishkel, R., Boyer, J., Tearpock, D., 2005. Structural and Stratigraphic Development of Extensional Basins: A Case Study Offshore Deepwater Sarawak and Northwest Sabah, Malaysia, American Association of Petroleum Geologists, 2005 Convention, Calgary.

Tucholke, B.E., Sawyer, D.S., Sibuet, J.-C., 2007. Breakup of the Newfoundland-Iberia rift, in: Karner, G., Manatschal, G., Pinheiro, L.D. (Eds.), Imaging, Mapping and Modelling Continental Lithosphere Extension and Breakup. Geological Society of London Special Publication, London, pp. 9-46.

Tucholke, B.E., Sibuet, J.-C., 2007. Leg 210 Synthesis: Tectonic, Magmatic, and Sedimentary Evolution of the Newfoundland-Iberia Rift, in: Tucholke, B.E., Sibuet, J.-C., Klaus, A. (Eds.), Proceedings of the Ocean Drilling Program, Scientific Results, College Station, TX (Ocean Drilling Program), pp. 1-56.

Uchupi, E., 1989. The tectonic style of the atlantic mesozoic rift system. Journal of African Earth Sciences 8, 143-164.

Uliana, M.A., Biddle, K.T., 1987. Permian to Late Cenozoic evolution of Patagonia, main tectonic events, magmatic activity, and depositional trends, in: McKenzie, G.D. (Ed.), Gondwana six: Structure, Tectonics, and Geophysics. AGU Monograph, Washington, D.C., pp. 271-286.

Uliana, M.A., Biddle, K.T., Cerdan, J., 1989. Mesozoic extension and the formation of Argentine sedimentary basins, in: Tankard, A.J., Balkwill, H.R. (Eds.), Extensional tectonics and stratigraphy of the North Atlantic margins, *AAPG Memoir* **46**, American Association of Petroleum Geologists, pp. 599-614.

Vail, P.R., Mitchum Jr., R.M., Todd, R.G., Widmier, J.M., Thompson III, S., Sangree, J.B., Bubb, J.N., Hatlelid, W.G., 1977. Seismic stratigraphy and global changes of sealevel, in: Payton, C.E. (Ed.), Seismic Stratigraphy - Applications to Hydrocarbon Exploration. AAPG Memoir pp. 49-212.

van Wijk, J.W., Huismans, R.S., ter Voorde, M., Cloetingh, S.A.P.L., 2001. Melt generation at volcanic continental margins: No need for a mantle plume? Geophysical Research Letters 28, 3995-3998.

Vinogradov, V.A., Gusev, E.A., Lopatin, B.G., 2003. Structure of the Eastern Arctic Shelf, Fouth International Conference on Arctic Margins ICAM IV. U.S. Department of the Interior - MMS Minerals Management Service, Dartmouth, Canada, pp. 90-98.

Wang, T.K., Chen, M.-K., Lee, C.-S., Xia, K., 2006. Seismic imaging of the transitional crust across the northeastern margin of the South China Sea. Tectonophysics 412, 237-254.

White, R., McKenzie, D., 1989. Magmatism at Rift Zones: The Generation of Volcanic Continental Margins and Flood Basalts. Journal of Geophysical Research 94, 7685-7729.

White, R.S., 1989. Initiation of the Iceland plume and opening of the North Atlantic. Extensional tectonics and stratigraphy of the North Atlantic margins, 149-154.

White, R.S., McKenzie, D., O'Nions, R.K., 1992. Oceanic crustal thickness from seismic measurements and rare earth element inversions. Journal of Geophysical Research 97, 19 683-619 715.

White, R.S., Smith, L.K., Roberts, A.W., Christie, P.A.F., Kusznir, N.J., Team, t.i., 2008. Lower-crustal intrusion on the North Atlantic continental margin. Nature 452, 460-465.

White, R.S., Spence, G.D., Fowler, S.R., McKenzie, D.P., Westbrook, G.K., Bowen, A.N., 1987. Magmatism at rifted continental margins. Nature 330, 439-444.

Whitmarsh, R.B., Manatschal, G., Minshull, T.A., 2001. Evolution of magma-poor continental margins from rifting to seafloor spreading. Nature 413, 150-154.

Williams, G.D., 1993. Tectonics and seismic sequence stratigraphy: an introduction, in: Williams, G.D., Dobb, A. (Eds.), Tectonics and Seismic Sequence Stratigraphy. Geological Society Special Publication, pp. 1-13.

Wilson, J.T., 1963. Evidence from islands on the spreading of the ocean floor. Nature 197, 536-538.

Wilson, M., 1992. Magmatism and continental rifting during the opening of the South Atlantic Ocean: a consequence of Lower Cretaceous super-plume activity? , in: Storey, B.C., Alabaster, T., Pankhurst, R.J. (Eds.), Magmatism and the Causes of Continental Break-up. Spec. Publ.-Geol. Soc. London, London, pp. 155- 241.

Wilson, R.C.L., Whitmarsh, R.B., Froitzheim, N., Taylor, B., 2001. Introduction: the land and sea approach, Geological Society, London, Special Publications, pp. 1-8.

Yan, P., Deng, H., Liu, H., Zhang, Z., Jiang, Y., 2006. The temporal and spatial distribution of volcanism in the South China Sea region. Journal of Asian Earth Sciences 27, 647-659.

Yan, P., Zhou, D., Liu, Z., 2001. A crustal structure profile across the northern continental margin of the South China Sea. Tectonophysics 338, 1-21.

Zhou, D., Ru, K., Chen, H.-z., 1995. Kinematics of Cenozoic extension on the South China Sea continental margin and its implications for the tectonic evolution of the region. Tectonophysics 251, 161-177.

Zhou, D., Yao, B., 2009. Tectonics and sedimentary basins of the South China Sea: Challenges and progresses. Journal of Earth Science 20, 1-12.

Zhou, X.M., Li, W.X., 2000. Origin of Late Mesozoic igneous rocks in Southeastern China: implications for lithosphere subduction and underplating of mafic magmas. Tectonophysics 326, 269-287.

Ziegler, P.A., Cloetingh, S., 2004. Dynamic processes controlling evolution of rifted basins. Earth-Science Reviews 64, 1-50.

- Reevaluation of volcanism during rifting and continental breakup
- Magma-poor and volcanic rifted end-member margin types are discussed
- The Laptev Sea, the South China Sea and the southernmost South Atlantic
- Implications on the formation of rift-onset and breakup unconformities
- A major controlling mode of hot-spot related mantle processes cannot be observed

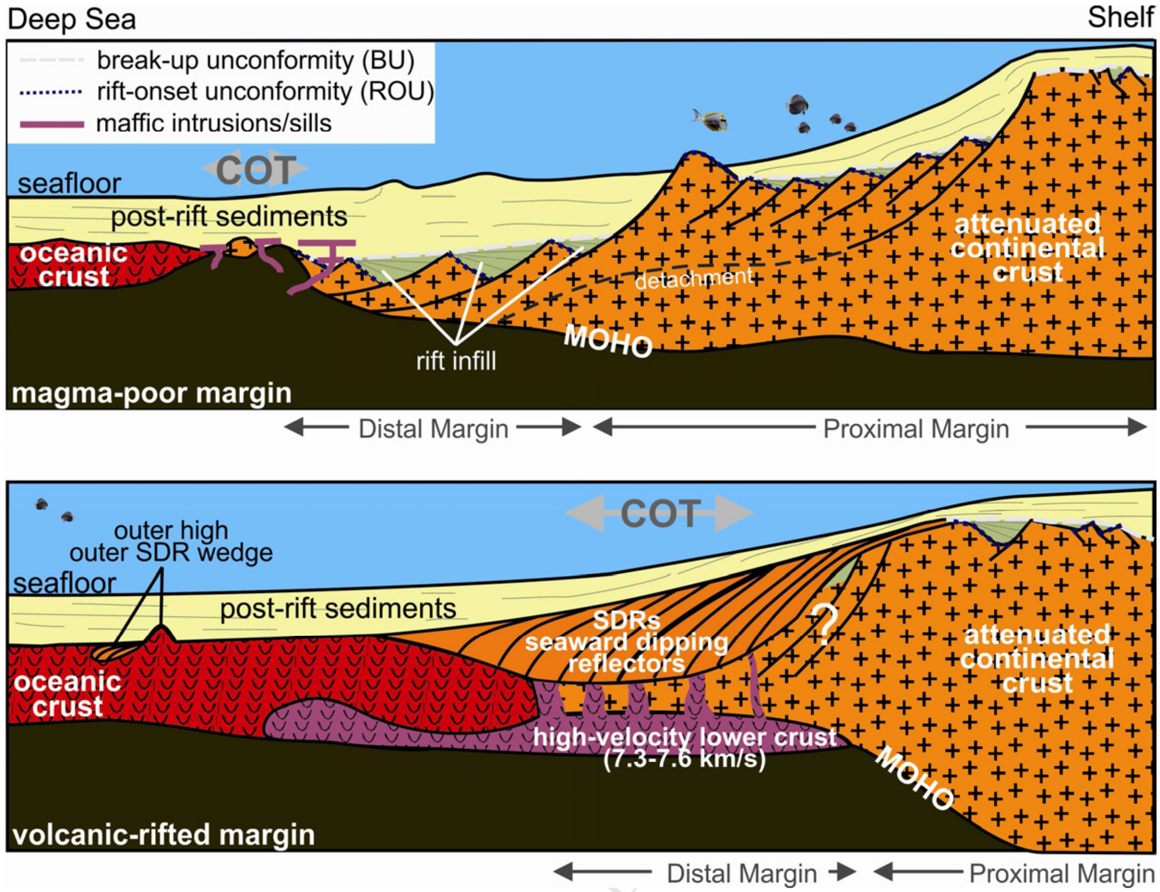
Deep Sea
Shelf
break-up unconformity (BU)
rift-onset unconformity (ROU)
maffic intrusions/sills
COT
seafloor
post-rift sediments
oceanic crust
detachment
attenuated continental crust
rift infill
MOHO
magma-poor margin
Distal Margin
Proximal Margin
COT
outer high
outer SDR wedge
seafloor
post-rift sediments
SDRs seaward dipping reflectors
?
attenuated continental crust
oceanic crust
high-velocity lower crust (7.3-7.6 km/s)
MOHO
volcanic-rifted margin
Distal Margin
Proximal Margin

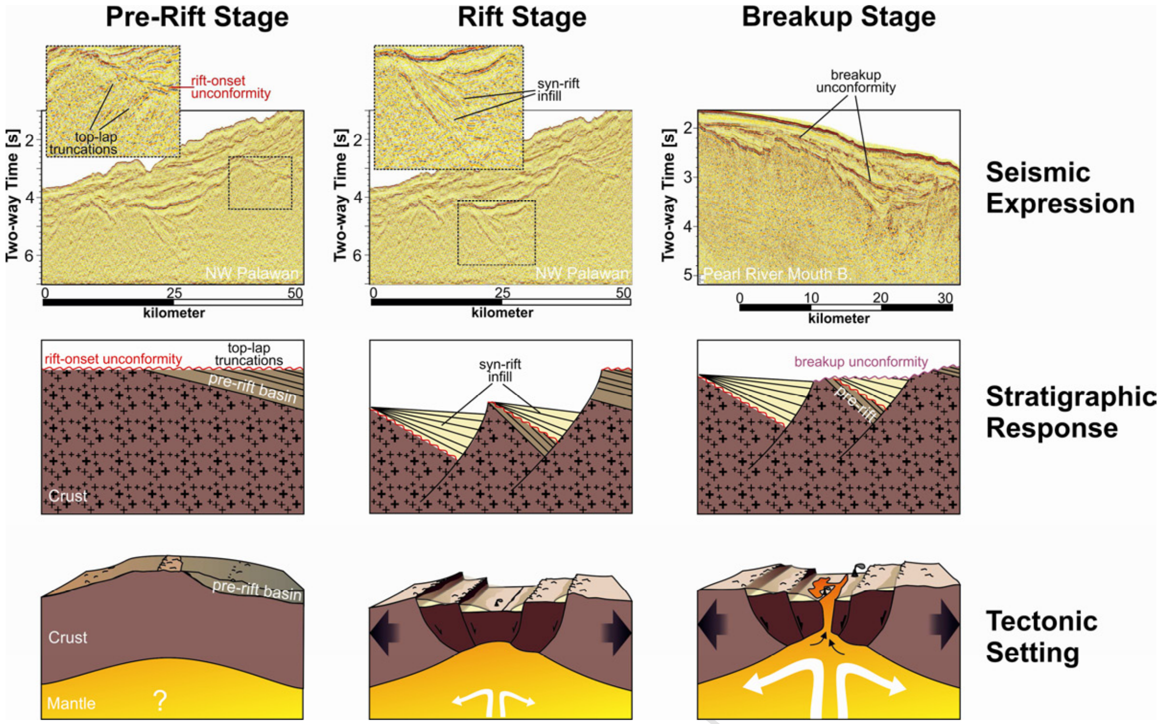

Pre-Rift Stage
Rift Stage
Breakup Stage
rift-onset unconformity
top-lap truncations
syn-rift infill
breakup unconformity
Two-way Time [s]
NW Palawan
Pearl River Mouth B.
kilometer
Seismic Expression
rift-onset unconformity
top-lap truncations
pre-rift basin
Crust
syn-rift infill
breakup unconformity
pre-rift
Stratigraphic Response
pre-rift basin
Crust
Mantle
?
Tectonic Setting

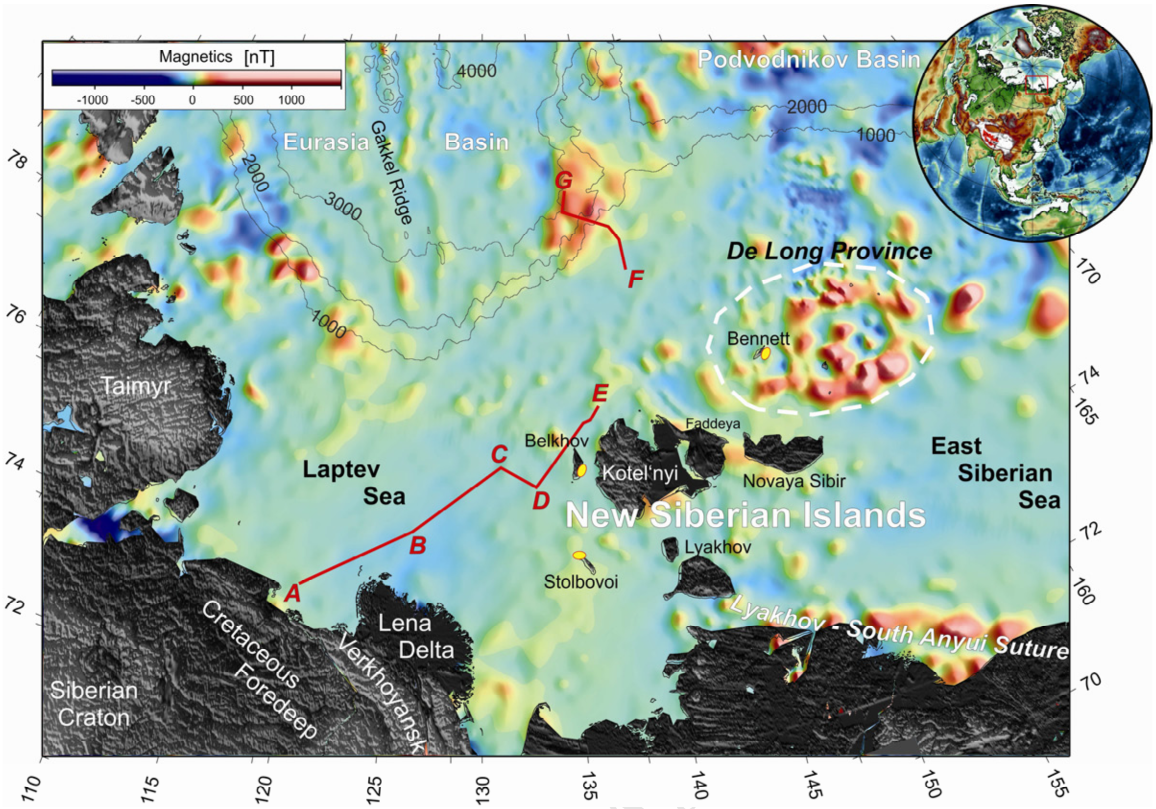

Magnetics [nT]
-1000 -500 0 500 1000
Podvodnikov Basin
4000
2000
1000
Eurasia
Gakkel Ridge
Basin
2000
3000
1000
G
F
De Long Province
Bennett
Taimyr
E
Faddeya
Belkhov
Kotel'nyi
Novaya Sibir
East
Siberian
Sea
C
Laptev
Sea
D
New Siberian Islands
B
Lyakhov
Stolbovoi
A
Lyakhov - South Anyui Suture
Lena
Delta
Cretaceous
Foredeep
Verkhoyansk
Siberian
Craton
78
76
74
72
170
165
160
110
115
120
125
130
135
140
145
150
155

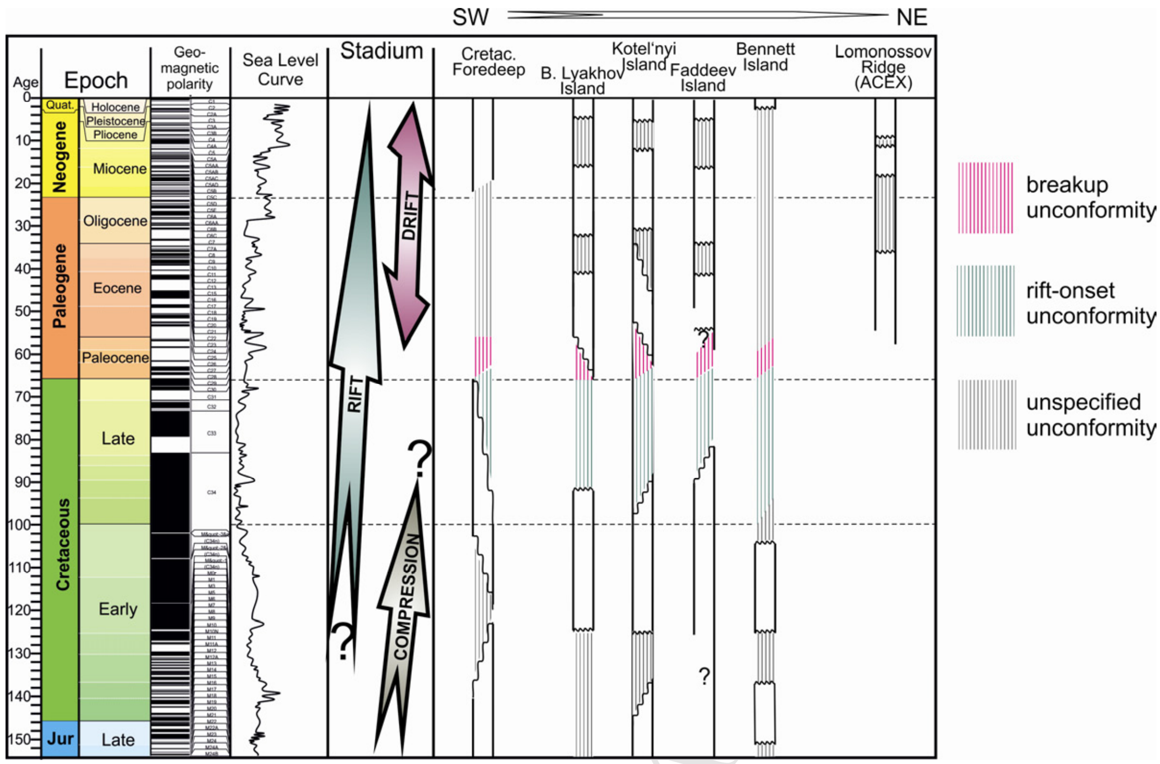
SW
NE
Age
Epoch
Geo-magnetic polarity
Sea Level Curve
Stadium
Cretac. Foredeep
B. Lyakhov Island
Kotel'nyi Island
Faddeev Island
Bennett Island
Lomonossov Ridge (ACEX)
Quat.
Holocene
Pleistocene
Pliocene
Neogene
Miocene
Oligocene
Paleogene
Eocene
Paleocene
Cretaceous
Late
Early
Jur
Late
RIFT
DRIFT
COMPRESSION
breakup unconformity
rift-onset unconformity
unspecified unconformity

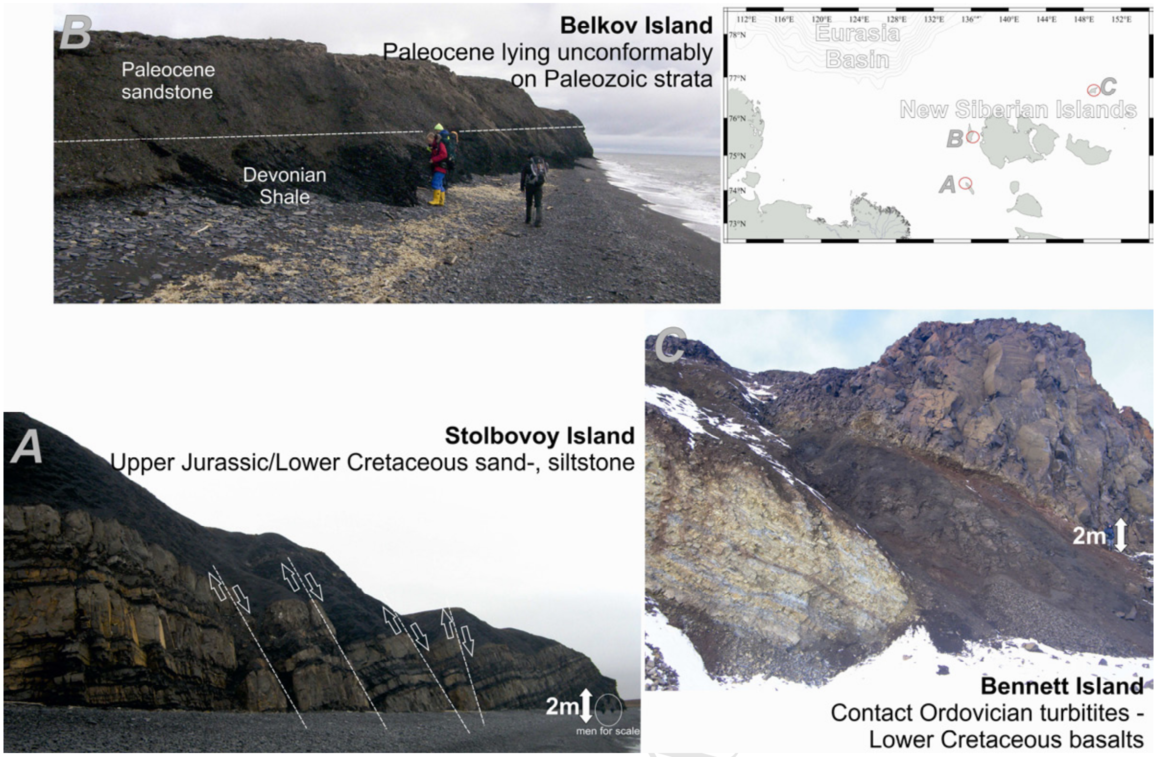
B
Belkov Island
Paleocene lying unconformably
on Paleozoic strata
Paleocene
sandstone
Devonian
Shale
Eurasia
Basin
New Siberian Islands
B
A
C
A
Stolbovoy Island
Upper Jurassic/Lower Cretaceous sand-, siltstone
2m
men for scale
C
2m
Bennett Island
Contact Ordovician turbitites -
Lower Cretaceous basalts

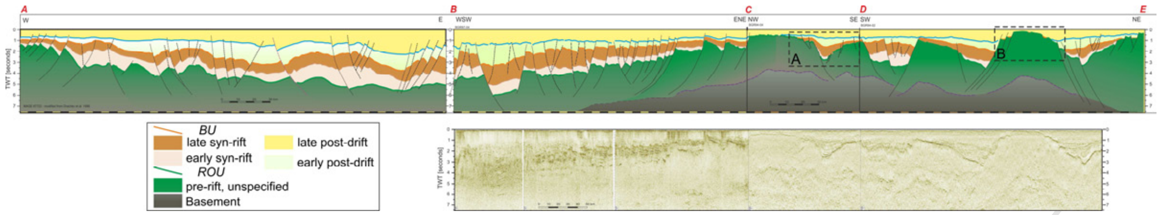
A
B
C
D
E
W
E
WSW
ENE NW
SE SW
NE
TWT [seconds]
BU
late syn-rift
early syn-rift
ROU
pre-rift, unspecified
Basement
late post-drift
early post-drift

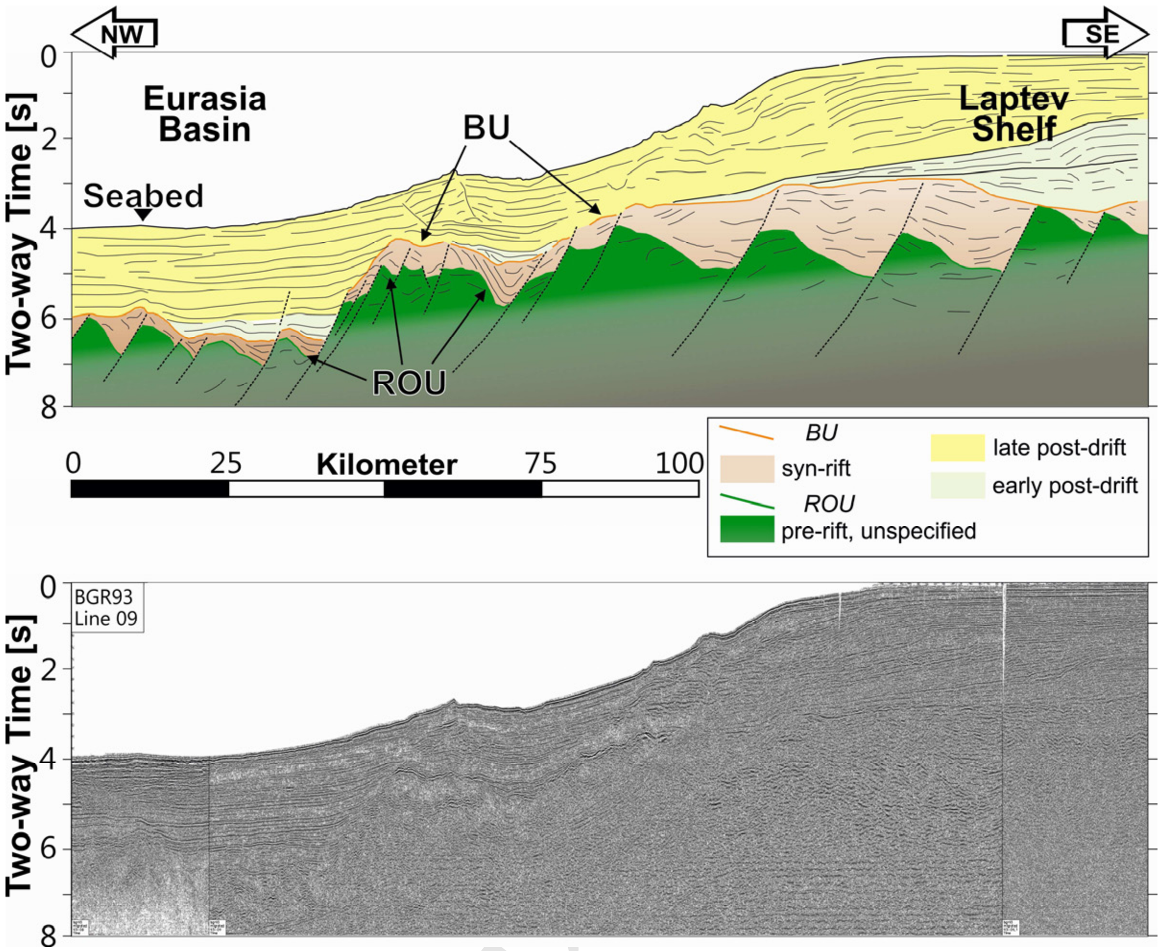
NW
SE
Two-way Time [s]
0
2
4
6
8
Eurasia Basin
Laptev Shelf
Seabed
BU
ROU
0
25
Kilometer
75
100
BU
syn-rift
ROU
pre-rift, unspecified
late post-drift
early post-drift
BGR93
Line 09

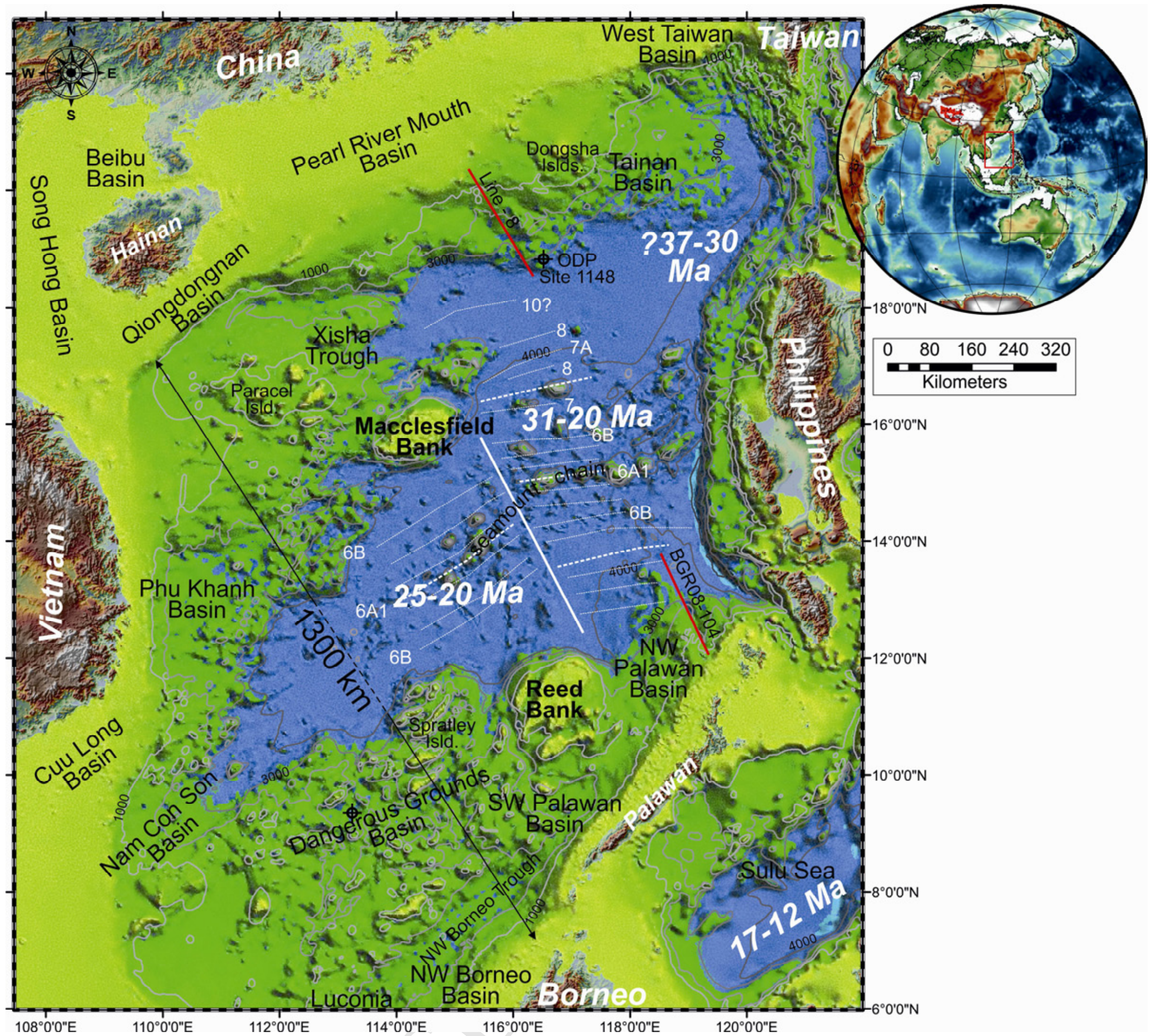

China
West Taiwan
Basin
Taiwan
Pearl River Mouth
Basin
Beibu
Basin
Song Hong Basin
Hainan
Dongsha
Islds.
Tainan
Basin
Line 8
ODP
Site 1148
?37-30
Ma
Qiongdongnan
Basin
Xisha
Trough
Paracel
Isld.
Macclesfield
Bank
31-20 Ma
Seamount chain
Philippines
Vietnam
Phu Khanh
Basin
25-20 Ma
1300 Km
BGR08-104
NW
Palawan
Basin
Reed
Bank
Spratley
Isld.
Cuu Long
Basin
Nam Con Son
Basin
Dangerous Grounds
Basin
SW Palawan
Basin
Palawan
Sulu Sea
17-12 Ma
NW Borneo Trough
NW Borneo
Basin
Luconia
Borneo
0 80 160 240 320
Kilometers
108°0'0"E
110°0'0"E
112°0'0"E
114°0'0"E
116°0'0"E
118°0'0"E
120°0'0"E
18°0'0"N
16°0'0"N
14°0'0"N
12°0'0"N
10°0'0"N
8°0'0"N
6°0'0"N

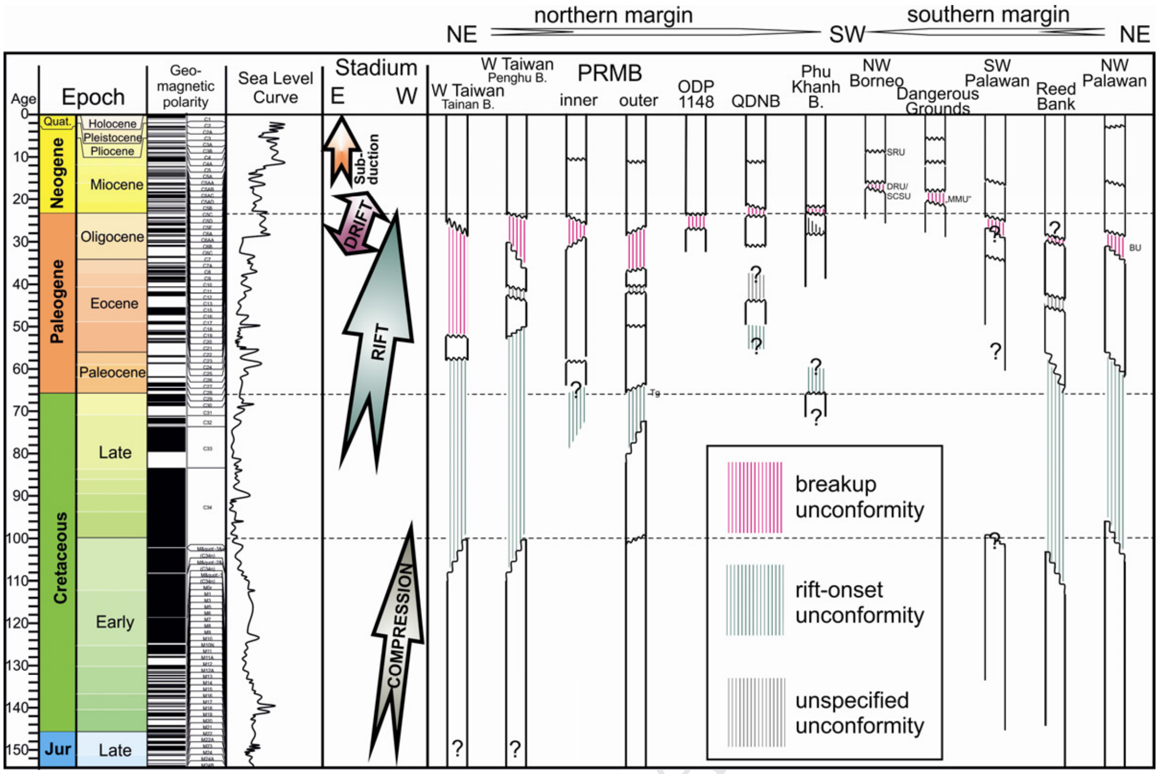

NE northern margin SW southern margin NE
Age
Epoch
Geo-magnetic polarity
Sea Level Curve
Stadium
E W
W Taiwan Tainan B.
W Taiwan Penghu B.
PRMB
inner
outer
ODP 1148
QDNB
Phu Khanh B.
NW Borneo
Dangerous Grounds
SW Palawan
Reed Bank
NW Palawan
Quat.
Holocene
Pleistocene
Pliocene
Neogene
Miocene
Paleogene
Oligocene
Eocene
Paleocene
Cretaceous
Late
Early
Jur
Late
Sub-duction
DRIFT
RIFT
COMPRESSION
SRU
DRU/ SCSU
„MMU"
BU
Tg
breakup unconformity
rift-onset unconformity
unspecified unconformity

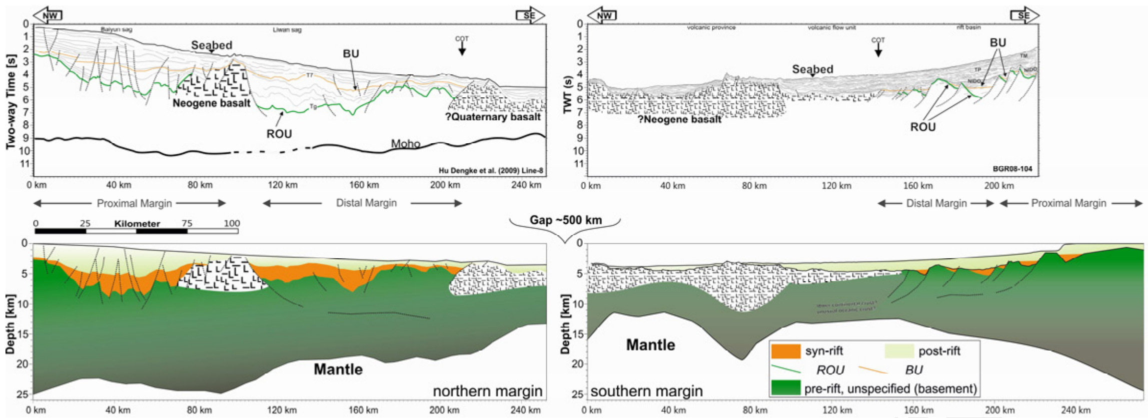
NW
SE
Baiyun sag
Liwan sag
COT
Seabed
BU
Neogene basalt
ROU
?Quaternary basalt
Moho
Two-way Time [s]
Hu Dengke et al. (2009) Line-8
Proximal Margin
Distal Margin
Kilometer
Gap ~500 km
volcanic province
volcanic flow unit
rift basin
?Neogene basalt
TWT (s)
BGR08-104
Distal Margin
Proximal Margin
Depth [km]
Mantle
northern margin
southern margin
syn-rift
post-rift
ROU
BU
pre-rift, unspecified (basement)

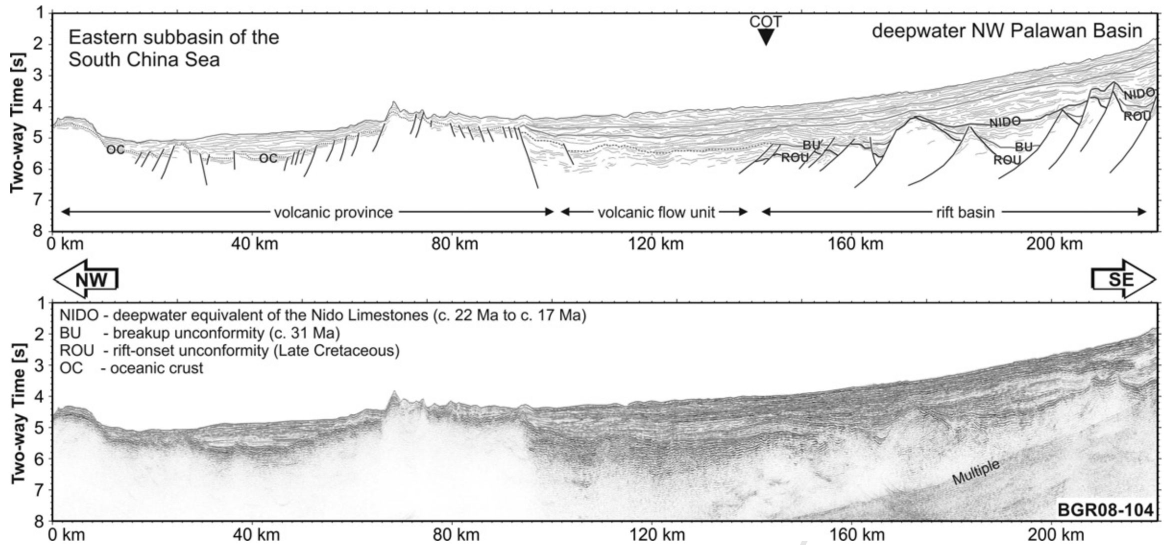

Eastern subbasin of the South China Sea
COT
deepwater NW Palawan Basin
Two-way Time [s]
OC
NIDO
ROU
BU
volcanic province
volcanic flow unit
rift basin
0 km
40 km
80 km
120 km
160 km
200 km
NW
SE
NIDO - deepwater equivalent of the Nido Limestones (c. 22 Ma to c. 17 Ma)
BU - breakup unconformity (c. 31 Ma)
ROU - rift-onset unconformity (Late Cretaceous)
OC - oceanic crust
Multiple
BGR08-104

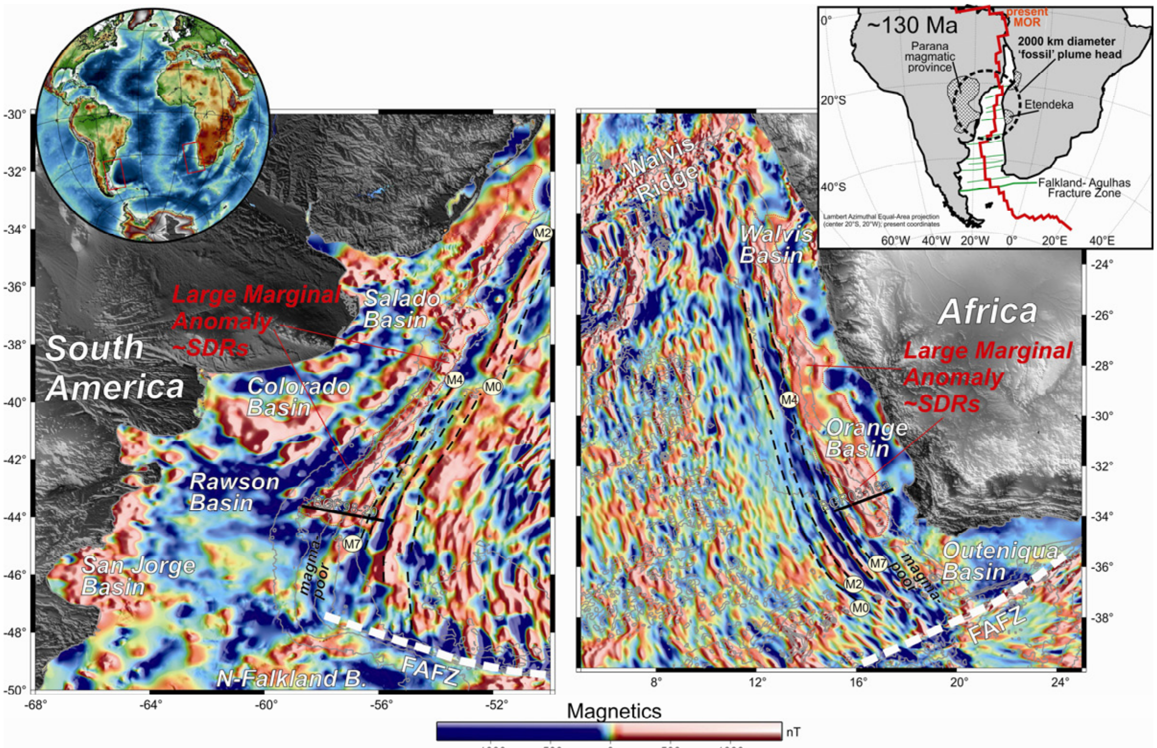
~130 Ma
present MOR
Parana magmatic province
2000 km diameter 'fossil' plume head
Etendeka
Falkland- Agulhas Fracture Zone
South America
Africa
Large Marginal Anomaly ~SDRs
Salado Basin
Colorado Basin
Rawson Basin
San Jorge Basin
N-Falkland B.
FAFZ
magma-poor
Walvis Ridge
Walvis Basin
Orange Basin
Outeniqua Basin
M0
M2
M4
M7
Magnetics
nT

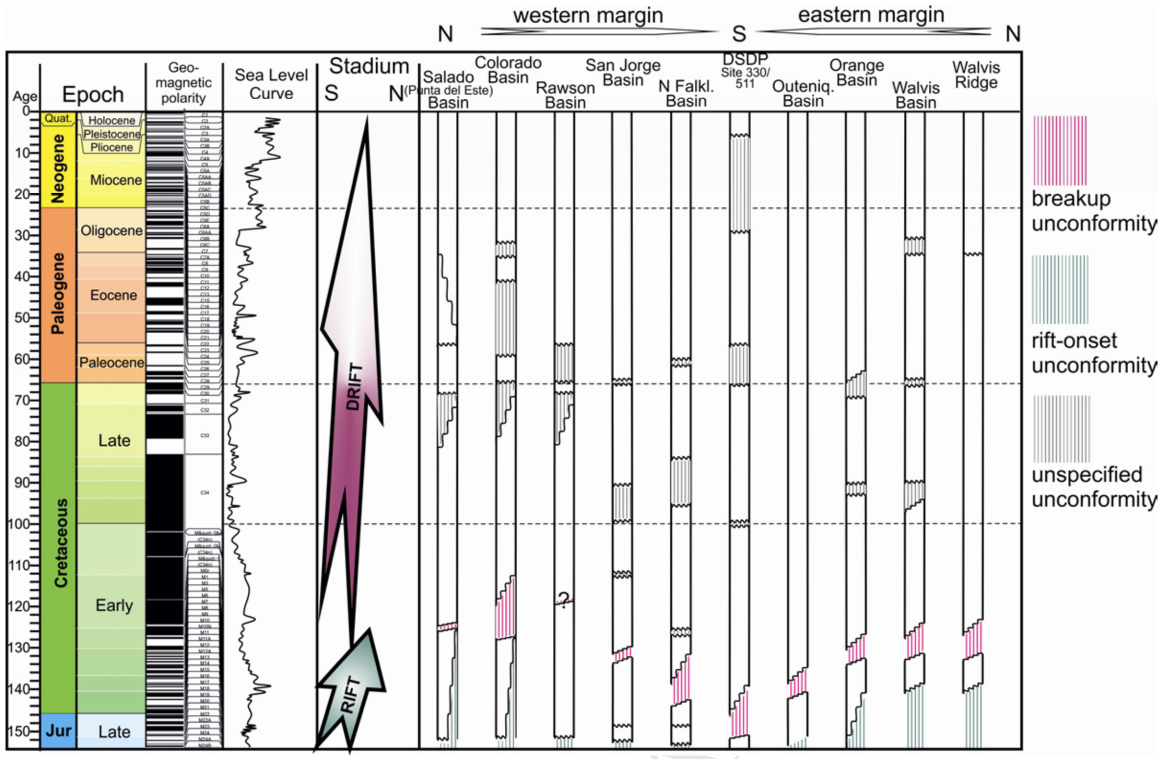

western margin
eastern margin
N
S
N
Age
Epoch
Geo-magnetic polarity
Sea Level Curve
Stadium
S
N
Salado (Punta del Este) Basin
Colorado Basin
Rawson Basin
San Jorge Basin
N Falkl. Basin
DSDP Site 330/511
Outeniq. Basin
Orange Basin
Walvis Basin
Walvis Ridge
Quat.
Neogene
Paleogene
Cretaceous
Jur
Holocene
Pleistocene
Pliocene
Miocene
Oligocene
Eocene
Paleocene
Late
Early
Late
DRIFT
RIFT
breakup unconformity
rift-onset unconformity
unspecified unconformity

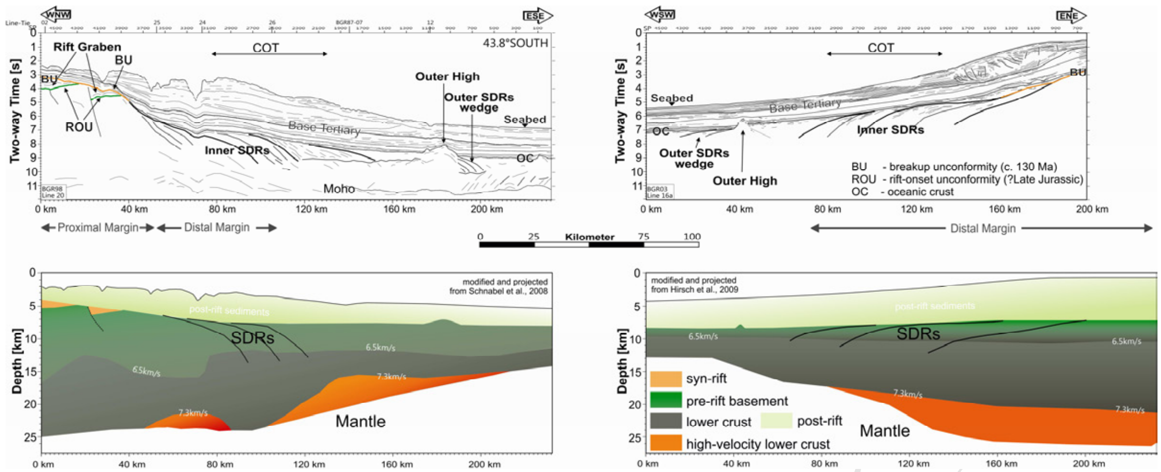

WNW
ESE
43.8°SOUTH
Rift Graben
BU
COT
Outer High
Outer SDRs wedge
Seabed
ROU
Base Tertiary
Inner SDRs
OC
Moho
Two-way Time [s]
Proximal Margin
Distal Margin
WSW
ENE
Seabed
Base Tertiary
Inner SDRs
Outer SDRs wedge
Outer High
BU - breakup unconformity (c. 130 Ma)
ROU - rift-onset unconformity (?Late Jurassic)
OC - oceanic crust
Kilometer
modified and projected from Schnabel et al., 2008
modified and projected from Hirsch et al., 2009
post-rift sediments
SDRs
6.5km/s
7.3km/s
Mantle
Depth [km]
syn-rift
pre-rift basement
lower crust
post-rift
high-velocity lower crust

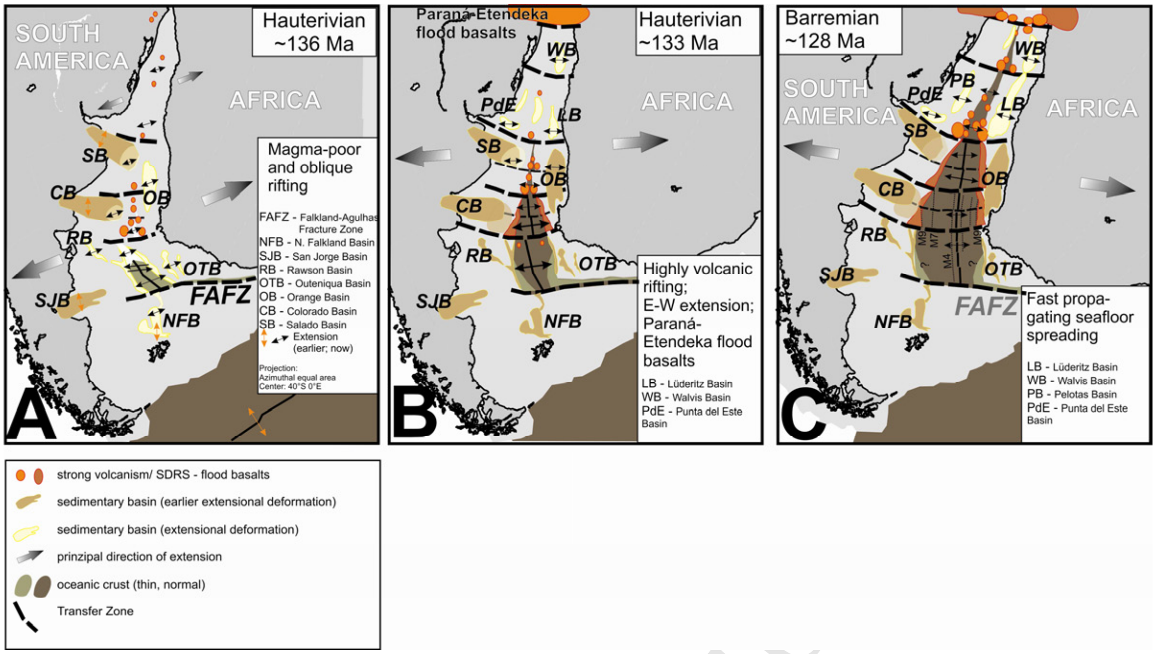

Hauterivian ~136 Ma
SOUTH AMERICA
AFRICA
Magma-poor and oblique rifting
FAFZ - Falkland-Agulhas Fracture Zone
NFB - N. Falkland Basin
SJB - San Jorge Basin
RB - Rawson Basin
OTB - Outeniqua Basin
OB - Orange Basin
CB - Colorado Basin
SB - Salado Basin
Extension (earlier; now)
Projection: Azimuthal equal area Center: 40°S 0°E
SB
CB
OB
RB
OTB
FAFZ
SJB
NFB
A
Paraná-Etendeka flood basalts
Hauterivian ~133 Ma
WB
PdE
LB
AFRICA
SB
OB
CB
RB
OTB
SJB
NFB
Highly volcanic rifting; E-W extension; Paraná-Etendeka flood basalts
LB - Lüderitz Basin
WB - Walvis Basin
PdE - Punta del Este Basin
B
Barremian ~128 Ma
SOUTH AMERICA
AFRICA
WB
PB
PdE
LB
SB
CB
OB
RB
SJB
OTB
NFB
FAFZ
Fast propagating seafloor spreading
LB - Lüderitz Basin
WB - Walvis Basin
PB - Pelotas Basin
PdE - Punta del Este Basin
C
strong volcanism/ SDRS - flood basalts
sedimentary basin (earlier extensional deformation)
sedimentary basin (extensional deformation)
prinzipal direction of extension
oceanic crust (thin, normal)
Transfer Zone

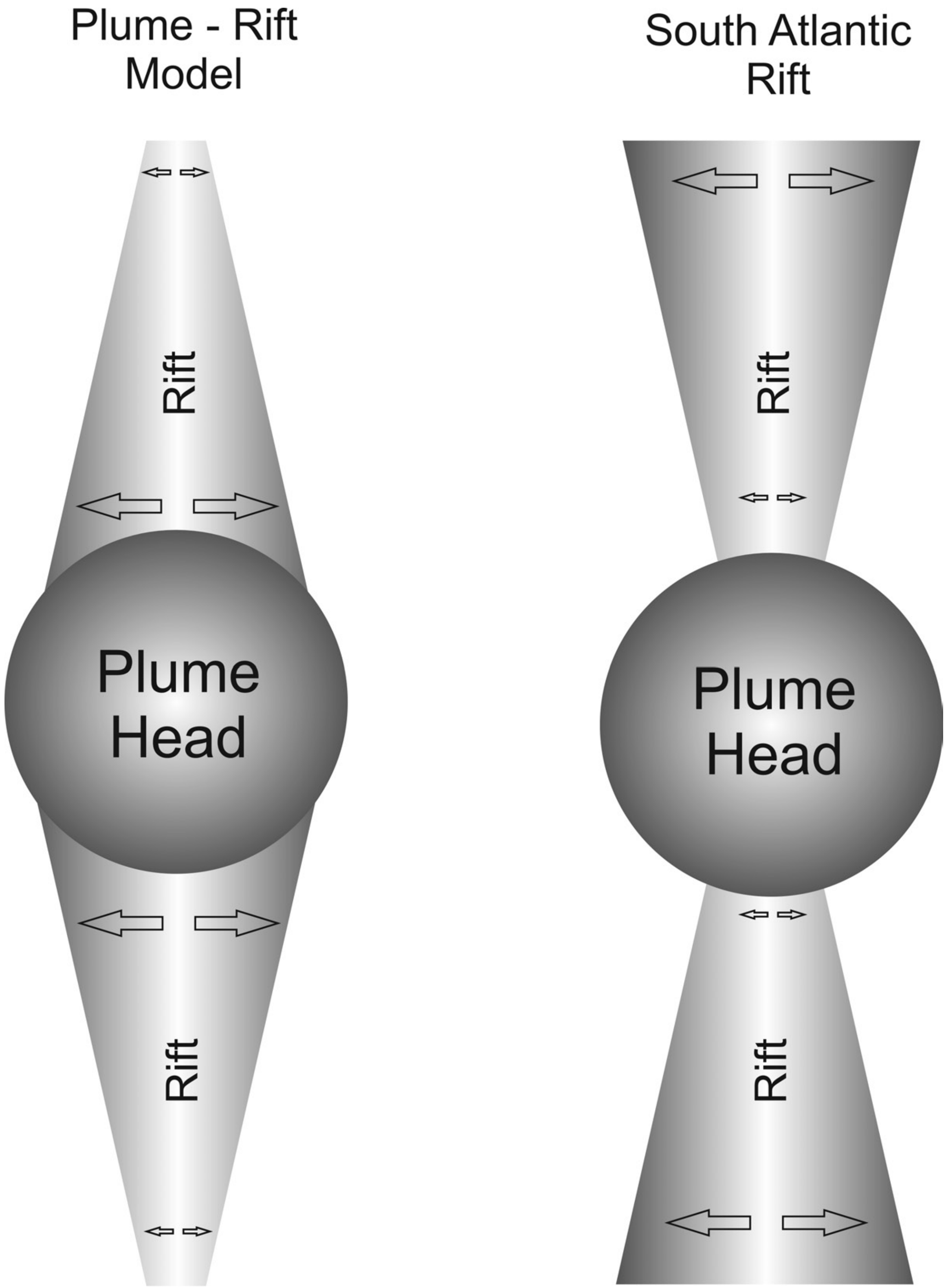
Plume - Rift
Model
South Atlantic
Rift
Rift
Rift
Plume
Head
Plume
Head
Rift
Rift

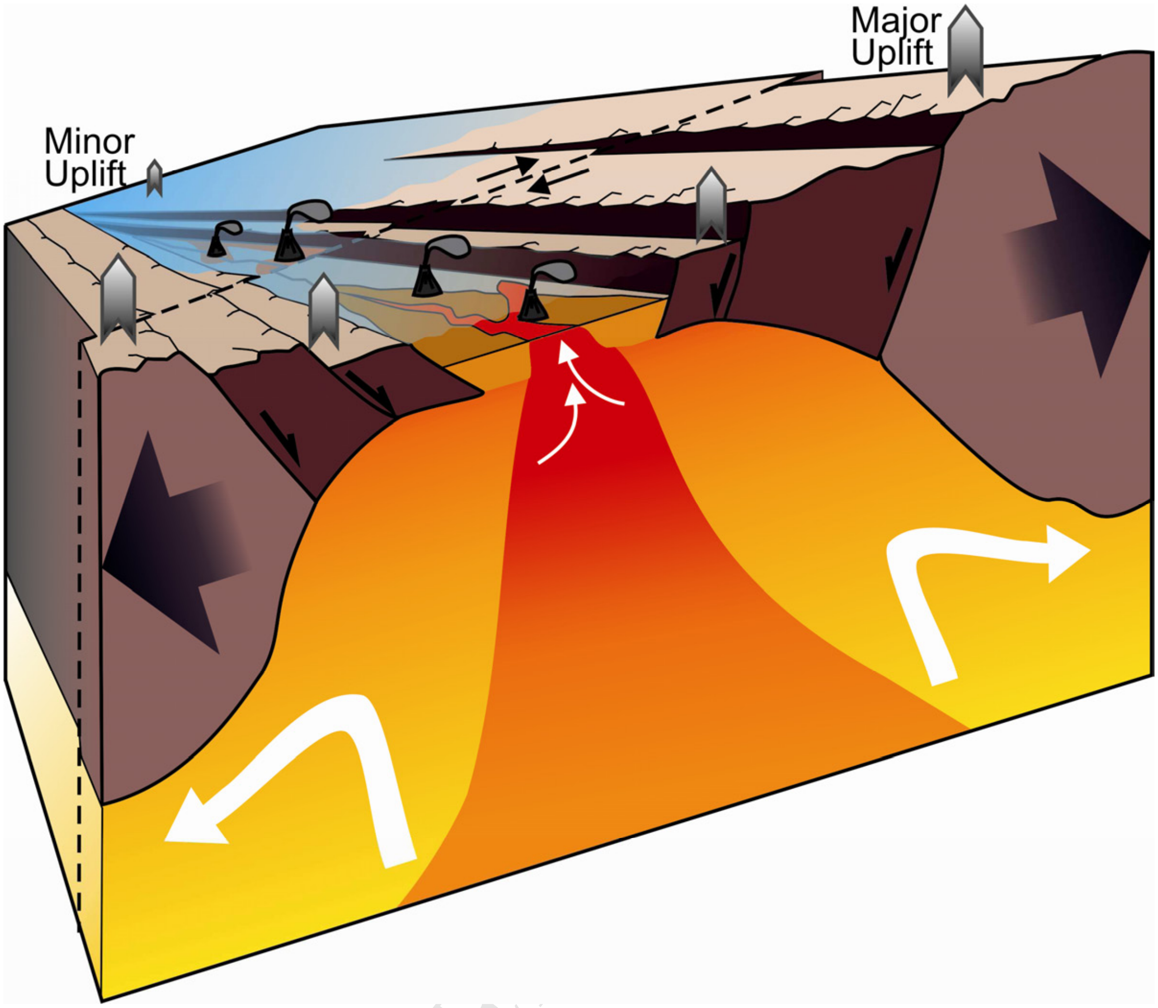

Major
Uplift
Minor
Uplift